Met O (APR) Turbulence and Diffusion Note No. 214

The Cardington stable boundary layer experiment 1993

by

S.H.Derbyshire, MRU Cardington

28 October 1994

Headquarters, Bracknell

Met O (APR) Turbulence and Diffusion Note No. 214

The Cardington stable boundary layer experiment 1993

by

S.H.Derbyshire, MRU Cardington

28 October 1994

Met O (APR)
(Atmospheric Processes Research)
Meteorological Office
London Road
Bracknell
Berks, RG12 2SZ

Note

Met O (APR) TDN-214

The Cardington stable boundary layer experiment 1993

S.H.Derbyshire, MRU Cardington

The Cardington stable boundary layer experiment 1993

S.H.Derbyshire, MRU Cardington

28 October 1994

Abstract

The Cardington stable experiment of 1993 is described, and results from the tethered-balloon/turbulence probe system presented. Results are basically consistent with the more limited Cardington data shown in Derbyshire (1994), and in most respects with recent Large Eddy Simulation. In particular, nondimensional mixing-lengths show a fairly sharp cutoff near a gradient Richardson number of 0.25, provided that quality control is imposed to ensure that the Richardson number is measured reasonably accurately. Many cases resemble idealized model boundary layers, e.g. with wind veering with height by 40°, but on the more stable occasions there is some evidence for local drainage effects. Intermittency in turbulence amplitude within 1-hour runs is found frequently below 50m.

1 Introduction

Stably-stratified atmospheric boundary layers are widely regarded as poorly understood. Some uncertainties relate to sensitivities to small slopes or low relief (e.g. Derbyshire and Wood 1994, Grant 1994 and references in those papers). However recent advances in describing neutral turbulent flow over hills via orographic roughness lengths z_0^{eff} highlight the potential combined impact of stratification and topography, and return attention to the uncertainties about even the most idealized stable boundary layers.

At both ECMWF and UKMO, SBL parametrization is recognized as a problem. Current parametrizations are thought to give too much turbulence at higher stabilities, at least in certain cases, leading to excessively deep nocturnal boundary layers. Boundary layer depth is important not least because of the impact on low cloud. However parametrizations which do cut off turbulence at higher stabilities (normally measured by the gradient Richardson number R_i), seem often to give unrealistic decoupling of layers. Dr A.Beljaars (personal communication) has speculated that additional mechanisms may need to be incorporated. Given such uncertainty, the empirical evidence needs to be strengthened or reconsidered.

In some models coarse vertical resolution may also be a significant weakness, but it is desirable to separate the resolution and parametrization issues conceptually. Different NWP models have very different vertical (as well as horizontal) resolutions, and the

resolution issue can be addressed by running one-dimensional 'single-column' models at varying resolution. All of this rests however on a reasonably accurate knowledge of the true 'physics'.

Recent advances in Large Eddy Simulation (e.g. Brown *et al.* 1994) are encouraging as a basis for parametrization, even though the stable case appears one of the most difficult to simulate because of the small turbulence length-scales. However validation requires detailed turbulence measurement across the boundary layer which is generally lacking from the existing literature. Stable boundary layers often show large gradients of wind and potential temperature, and these gradients are not generally concentrated in the surface layer in the manner typical of neutral or convective boundary layers. Hence a programme of direct turbulence measurement across the whole stable boundary layer, combined with accurate measurement of gradients, is potentially very valuable.

In analyzing results from previous MRU detachments in heterogeneous terrain it was realized that comparison with a more 'ideal' site, e.g. Cardington, was necessary as a 'control', and a series of nocturnal balloon flights was carried out in early 1993, as will now be described.

The Cardington site, though open and away from orography, lies in gently rolling terrain unlike the plains of Minnesota (Caughey *et al.* 1979). A detailed description and map is given by Grant (1994), the most significant feature being a modest ridge up to about 50m above site, oriented roughly NE-SW and located some 2.5km to the southwest. This implies a mean slope of roughly 2/100 between ridge-top and site.

However for purposes of stable boundary layer measurement the difference between Cardington and Minnesota is less than at first appears. Arguments of Derbyshire and Wood (1994) imply that the total elevation change over quite a long fetch is more relevant than the slope, i.e. long gentle slopes can be as effective in generating drainage effects as shorter steeper slopes. If the drag coefficient c_d is not strongly perturbed by local effects, the appropriate fetch can be estimated as z/c_d. The fetch for the boundary layer as a whole to adjust to the underlying topography is $h/c_d \sim G/|f| \sim$ 100km typically, where h is boundary layer depth, G geostrophic wind and f Coriolis parameter. This estimate can be inferred from the overall momentum balance or in more detail from a quasi-steady boundary layer model (Derbyshire 1990). Essentially, because the idealized boundary layer is in balance between turbulence and Coriolis/inertial effects, the turbulent adjustment timescale is comparable with the Coriolis timescale. These arguments therefore imply that for stable boundary layer purposes the 'flatness' of a site needs to be considered over a wide area (further than the eye can see).

Derbyshire and Wood (1994) develop a simple argument to assess drainage effects from the baroclinic term in the vorticity equation. In the hydrostatic limit (horizontal scales $\gg$ vertical scales), horizontal vorticity approximates to wind-shear. If near the surface the isentropes (θ contours) are parallel to the ground, then to assess such effects the elevation change should be compared with the height-scale U/N. If, further, the stable surface layer lies close to a critical Richardson number R_{ic}, the scale U/N can be estimated as $z/R_{ic}^{1/2}$. As a rule of thumb, this suggests that stable flow at levels below the hill-top should be influenced by such effects even if the hill-top is rather distant, unless it is further than $O(z/c_d)$ away. Even above the hill-top level, the decay of such

influence is algebraic, not exponential, until and unless the isentropes flatten out with height. It should be noted however that the above argument is rather simplified; a more detailed analysis of stable flow over hills, albeit with restriction to small amplitude and moderate stability, has been developed by Belcher and Wood (1994).

Derbyshire (1994) argues that variability is one of the most urgent general issues in SBLs, because SBL variability is thought particularly large, and because of sensitivity to the gradient Richardson number R_i in particular.

2 Experimental Method

The quality of observations, or research experiments, depends on minimizing various errors. These may be divided loosely into two classes:

(i) measurement error (including not only direct sensing but also calibration, electronic and processing-software errors)

(ii) representativeness errors (the measurement might be locally correct, but poorly sited, averaged over inappropriate periods or otherwise unrepresentative of the intended variable).

Unfortunately measurement errors do not always follow the classical Gaussian probability distribution (cf. Dharssi *et al.* 1992, who consider occasional gross errors in operational measurements). Elimination, or at least detection, of gross errors is a key part of experimental technique. *Representativeness* is particularly important in research experiments, which seek to draw general conclusions from particular measurements.

The MRU tethered-balloon/turbulence-probe system, with software correction for cable motion, is described in Lapworth and Mason (1988). It is well suited to stable boundary layer measurement, avoiding the problems of aircraft and tower measurement (need for very fast response, flow distortion etc.).

The instrument package is essentially the turbulence probe described in Lapworth and Mason (1988). Three Gill polystyrene propeller anemometers in a 60° cone give fast-response wind-components. The Gill length constant ~1m is the main response limitation. A wind-vane on the probe tail keeps the probe pointing roughly into wind. A platinum resistance thermometer (PRT) is deployed on a stalk along the cone axis. The probe measures its own orientation using inclinometers and magnetometers, and this information is also used to reconstruct the cable motion. The probe also incorporates a pressure sensor for altimetry and other purposes. The main changes from the Lapworth-Mason design are an improved shielding for the slow thermistor, and the incorporation of a humicap relative humidity sensor.

The various sensors provide an analogue voltage output, which is then electronically conditioned (filtered/scaled) using operational amplifiers, before being multiplexed, digitized, encoded into error-correcting Manchester code, passed to a transmitter in the meteorological (400-406MHz) band and finally telemetered to a ground-station and thence to a MicroVax minicomputer for logging at 4 Hz (although sampling at 20 Hz).

The probe system is electronically complex. Occasional problems have been found with temperature signals, particularly from the fast PRT, which sometimes shows spikes leading to a white noise component in the power spectrum. A despiking algorithm was run on the PRT channel. Upper estimates of the proportion of temperature variance associated with 'grid-scale noise' were typically 10%, consistent with normal inertial-subrange scaling. Only one gross contamination (> 20%) was found and the point removed from analysis. After the 1993 stable experiment, changes to the probe electronics and earthing arrangements were made and seemed to reduce vulnerability to such problems. Mean temperatures were calculated using the slow thermistor.

Flights on 7 stable evenings will be described. Some further flights were conducted for other purposes. A couple of flights were not considered in detail because the wind direction was too close to obstructions. On each flight around 8 probes were flown, giving typically 4-5 hrs turbulence data. In stable conditions turbulence length-scales are generally small enough that no two probes will sample the same eddy. Eddy timescales are also relatively short. As will be shown, this quantity of data enables us to apply relatively stringent quality-control and draw statistically significant conclusions on many points relevant to modellers. Level (turbulence) runs were generally 1-hour in duration (plus a few half-hour runs). Standard linear detrending was applied.

At the beginning and end of a flight, and sometimes during a flight, 'profile' runs were conducted, in which probes were raised or lowered sufficiently to intercompare calibrations.

Some surface data were logged separately but not in the same format, and the surface configuration was varied during the flying period. Here no detailed comparison will be attempted between surface and balloon measurements, nor to extend the climatology which Grant (1994) gives for Cardington using sodar and mast-based instruments. It will be seen later that turbulence profiles do not follow a simple standard form, and therefore there is an advantage in using direct turbulence measurements at height when these are available.

We shall interpret our measurements particularly in terms of the dependence of turbulence amplitude and structure on R_i. Unfortunately calculation of R_i is very vulnerable to calibration errors, which carries a real risk of systematic bias. A semi-objective smoothing algorithm was employed, as described in Derbyshire (1994) based on the instrumental tolerances, with the aim of removing the systematic impact of such measurement errors. The subjective element consists in prior expectations of profile shape or curvature. However some objective constraints can be imposed approximately by eye. For instance, if measurements lie consistently to one side of the smoothed curve then smoothing is probably excessive. Here the smoothing algorithm was applied after rough corrections based on intercomparisons during profile runs.

3 Results

Derbyshire (1994) discusses the difficulty of a complete comparison between individual boundary layer measurements and an idealized research model such as LES. Account

would need to be taken of mesoscale advection as well as probably other physical processes besides turbulence (e.g. soil heat diffusion). However we may consistently apply local scaling analyses, following Nieuwstadt (1984), which may be compared with LES. Mixing-lengths, another local quantity, relate directly to parametrizations in forecast models, and after suitable scaling may also be compared with LES. Validation of LES in such terms, even without a full profile comparison, would give considerable confidence. We shall also however consider indicators of whether or not turbulence is 'more variable' in atmospheric stable boundary layers than in idealized models.

First of all (Figs. 1-7), a compilation of profiles is shown for each flight, with a considerable variety in windspeed (U) and potential temperature (θ) profiles. Stability is shown via a monotonic function of R_i. In almost all cases, a 'normal' wind-veer with height of 30-40° develops by end of flying, in contrast to the Minnesota results of Caughey *et al.* (1979). After showing the basic profiles of mean wind, temperature, we show the turbulent fluxes which influence these mean profiles. Later we shall show local nondimensional plots with a view to both predicting turbulent fluxes from the mean profiles (e.g. for NWP purposes) and also comparison with Large Eddy Simulation (LES).

Symbols denote values 'as measured', curves results of the smoothing algorithm (applied only to mean values of the basic variables). Smoothing applied to wind-speed U is almost imperceptible, reflecting the high accuracy of this measurement. Corrections to wind direction were typically a couple of degrees. Corrections to $\overline{\theta}$ were typically 0.2K, although a few gross errors were seen and detected using profile runs.

The $\overline{q}$ profiles, where q is specific humidity, are included for completeness simply to give a rough idea of the humidity, but without intercomparisons or smoothing. Most of the $\overline{q}$ profiles show small kinks due to measurement errors, which are noticeable because there is generally little gradient in $\overline{q}$. The lack of $\overline{q}$-gradient reflects the absence of significant moisture fluxes: evening evapotranspiration from dry ground in January-March was low and flights normally ceased too early for substantial dewfall. In principle a 'virtual temperature' term in $\partial\overline{q}/\partial z$ should be incorporated in R_i, but here the correction is small (1g/kg corresponding to 0.2K in virtual temperature), and omitted because of the low signal-noise ratio in the humidity gradient. If, as usually assumed in models, sensible and latent heat are transported by turbulence at the same rate (i.e. $K_h = K_q$, where K_h and K_q are the respective eddy diffusivities), then the fractional contribution of moisture gradient to R_i is about $(13Bo)^{-1}$, where Bo is the Bowen ratio.

Profiles of eddy viscosity K_m are also included for completeness. Above the boundary layer these must be treated as very crude indications, with low confidence attached. It may be regarded also as an estimate for K_h aloft, for which the present measurements are not accurate enough to offer a direct estimate. Values of K_h in the free atmosphere are of some significance to modelling of pollution dispersion; if small but non-vanishing, they might enable scalars emitted from the surface to be diluted over a layer substantially deeper than the boundary layer as normally defined. The present measurements *suggest*, very tentatively, that whilst above a late-evening SBL K_m can fall as low as $10^{-2}\mathrm{m}^2\mathrm{s}^{-1}$ aloft, it is not necessarily lower than within the SBL itself. The associated Reynolds stress $|\tau|$ e.g. on 260393 can fall below $10^{-3}\mathrm{m}^2\mathrm{s}^2$.

So far we have shown 'unscaled' profiles. To draw general conclusions, we wish however to consider standard scalings, e.g. for mixing-length l_m in relation to height z and other variables. Fig. 8a shows non-dimensional mixing-length l_m/z against R_i based on a quality-control rejecting points with small shear, for which gradients are not accurately measured. A fairly sharp turbulence cutoff around $R_i = 0.25$ is found. Most of the points for $R_i < 0.15$ are in fact below 50m. The guideline is not a best fit, but a simple interpolation between $l_m/z = 0.4$ at neutral stability and 0 at $R_i = 0.25$.

Fig. 8b shows a slightly different nondimensionalization, using $z' = (1/z+0.4/0.15h)^{-1}$, where h is the estimated boundary layer depth. This 'Blackadar' nondimensionalization is consistent with the formulation in the UKMO Unified (forecast/climate) Model. The Blackadar nondimensionalization marginally improves agreement with the guideline, especially for points below 50m. Fig. 8c shows the very scattered results obtained without quality-control. It is easy to see that averaging without quality-control could lead to a spurious conclusion that significant turbulence can be maintained at high R_i. Such an empirical conclusion can be accepted only if R_i is reasonably accurately measured.

We shall now consider local scaling diagnostics which, though apparently esoteric in some cases, provide significant tests of both LES and 2nd-order closure models. The latter are significant as a basically rational approach, consistently handling energy conversions, from which by local approximations model parametrizations may be derived.

Fig. 9a shows the diagnostic $a_w^{-1} = |\tau|^{1/2}/\sigma_w$ from the present measurements, together with a curve derived from Brost and Wyngaard's (1978) second-order closure, which to some extent represents a fit to the Kansas surface-layer measurements. Apart from a couple of outliers, agreement is good, and even for $R_i > 0.25$ the closure appears, perhaps fortuitously, to mimic the observed fall-off in a_w^{-1}. This diagnostic is a significant check on turbulence measurements, partly because it seems to vary little with stability and is therefore less affected by the difficulty of measuring R_i. Furthermore any change to a different flow regime such as gravity waves would be expected to change a_w grossly.

Turbulence in stable boundary layers is often said to be 'intermittent', but the nature of such intermittency is not well understood, nor is it clear whether idealized simulations such as Brown *et al.* (1994) can or should capture intermittency. Furthermore evidence from operational anemometers, typically at 10m, should be treated cautiously because of their starting speed (typically 5 knots; I am grateful to Alan Grant for pointing this out).

There are two possible views of any such intermittency: (i) as a local process, presumably controlled by R_i; (ii) as a property of the boundary layer as a whole. Both Mahrt (1988) and Derbyshire (1990) take the latter view. Perhaps the simplest diagnostic for intermittency is the kurtosis of vertical velocity, $K[w] = \overline{w^4}/\sigma_w^4$, which is plotted (as a reciprocal) against R_i in Fig. 9b. A standard Gaussian value $1/K[w] = 1/3$, which may be taken as a baseline for 'non-intermittent' turbulence, is shown as a dotted line. Indeed all points lie below this line, though many only slightly. There is no very clear trend with R_i, except that the very highest stability points ($R_i > 0.4$) are more intermittent. The points in the range $0.25 < R_i < 0.35$ are not very intermittent. The clearest result is that nearly all of the points with $K[w] > 5$ lie in the lowest height-band, and

about half the points in that band show $K[w] > 5$.

Turbulent fluctuations of temperature or buoyancy are important not only because they are necessary for a turbulent heat flux, and hence in controlling the mean temperature profiles, but also because of their significance for the turbulent energy balance as a whole.

Various non-dimensional quantities associated with temperature or buoyancy fluctuations are shown in Fig. 10. For these plots the first run on each night was excluded, as this run was typically associated with transition in the surface flux; in fact this removed only a few points. Fig. 10a shows $\varsigma_\theta = \sigma_b/\sigma_w N$ where b is buoyancy ($b' \sim g\theta'/\theta$). In Fig. 10b, the same data are binned by R_i, with error bars showing standard error of the mean and isolated points indicated with square brackets. Apart from the (bracketed) isolated points, the Brost-Wyngaard (BW) curve is a good fit to the bin means. Brown *et al.* (1994) found at moderate stabilities ς_θ lying around 10% below BW. The present results deviate from BW by about 5% in the same sense. For $\mathcal{F} = -\overline{w'b'}/\sigma_w^2 N$ (Figs. 10c,d) the systematic deviation from BW is clearer. Brown *et al.* (1994) find $\mathcal{F}$ lying about 20% below BW's predictions at moderate stabilities ($R_i \simeq 0.2$), whereas the data lie about 30% below BW.

Theoretically, ς_θ^2 can be interpreted as the ratio of available potential energy (APE) associated with buoyancy fluctuations to the kinetic energy of vertical motions. The above results imply that these two forms of energy are comparable at moderate stabilities. $\mathcal{F}$ can be approximated to a rate of mixing of temperature fluctuations, nondimensionalized by the buoyancy frequency N.

For the negative correlation-coefficient $-r_{w\theta}$ between w and θ (Fig. 10e), the BW curve is a reasonable fit to the data. In fact the Brown *et al.* results with backscatter closely follow the BW curve, whereas the non-backscatter curve has a similar shape but about 30% lower. For $R_i \gtrsim 0.15$, the present data are slightly closer to the non-backscatter curve. Although the scatter is fairly large, on binning together points for $0.15 < R_i < 0.3$, the data lie about 3 standard errors (of the mean) below the BW and backscatter curves.

Fig. 11 shows (for 080393 only) ϵ, i.e. turbulence kinetic energy dissipation per unit mass, divided by the predictions of a formula due to Hunt and co-workers, namely $\epsilon = \sigma_w^3(0.26/z + 0.47S/\sigma_w)$, where S is the modulus of vector wind-shear. In the range $0 < R_i < 0.25$ fair agreement is obtained, with little obvious bias. For higher R_i, the formula may over-predict ϵ slightly. Here ϵ was estimated manually from spectra, and as yet only for 080393 because the procedure is rather time-consuming. It is intended to develop a reliable automated form of this manual procedure. Parametrization of ϵ is difficult but critical; the dissipation length-scale can be regarded as controlling all the other turbulence length-scales.

4 Conclusions

The Cardington 1993 stable experiment was focused on measurement of turbulence, including temperature fluctuations and fluxes, across the stable boundary layer using

the turbulence probe. The level of detail was broadly comparable with recent research simulations, although it was not possible (or really necessary) to match their high vertical resolution. Radiometers were employed, though regarded as a rough check only. The PRTs are treated with slight caution, because during this period the electronics were occasionally found to give spikes. Some of the temperature spectra show high-frequency contamination, but the effect on total variance was small. Some electronic changes were made subsequently.

A variety of nocturnal conditions was encountered, including some very clear nights but also some cloudy ones. Some cases approached a quasi-steady state, whereas others evolved in more complicated ways. Perhaps surprisingly however, nearly all flights developed a 'normal' wind-veer with height across the boundary layer of 30-40°, consistent with idealized models, although one light-wind case showed low-level backing with height which may have been influenced by drainage flow or other topographic effects.

Results from a clear and windy night, 080393, were previously written up (Derbyshire 1994) and contrasted with a flight at a more heterogeneous site. In general the results from the full Cardington dataset, scaled appropriately, are consistent with 080393, although that particular night is closest to the quasi-steady, continuously turbulent stable boundary layer suggested by idealized models.

In particular the conclusions from 080393 are borne out by the full dataset as regards the fairly sharp turbulence cutoff for $R_i > 0.25$, after quality-control rejecting small gradients which are not accurately measured. Without such quality-control results are very scattered, and naive averaging could lead to quite erroneous conclusions. The turbulence cutoff, shown by analysis of mixing-length l_m, has direct relevance to model parametrizations.

The full Cardington dataset shows more intermittency, at least near the surface, than does 080393, as diagnosed by the kurtosis of vertical velocity within 1-hour runs. This is again significant for models, as representing one kind of variability.

Various local-scaling diagnostics have been plotted against R_i. The diagnostic a_w^{-1}, in the surface layer equivalent to u_*/σ_w agreed well with the Brost-Wyngaard predictions. LES results of Brown *et al.* (1994) differ slightly but systematically. Two diagnostics for heat-transport, $\mathcal{F}$ and ς_θ, due originally to Hunt and co-workers and discussed by Mason and Derbyshire (1990), were also plotted against R_i. For these, the present data, like LES, give somewhat lower values than BW predict. There is reasonable agreement on the correlation coefficient $-r_{w\theta}$. The data agree with LES with backscatter at lower stabilities, although at higher R_i they are slightly closer to the non-backscatter LES.

These local-scaling quantities provide significant tests of LES and 2nd-order closure models even when the boundary layer as a whole does not match any idealized model.

For 080393 only, turbulence kinetic energy dissipation ϵ was estimated manually from spectra. (This procedure is laborious, although results are found to be credible.) From a limited quantity of data, overall agreement with a formula due to Hunt is reasonable, and does not suggest the need for an additional R_i-correction, except perhaps for $R_i > 0.25$.

Finally, it is worth reviewing the rationale for experiments of this kind, given recent advances in research modelling, e.g. Brown *et al.* (1994), with LES. Even by carefully

selecting flights such as 080393, it is hard to match the 'cleanness' of recent LES work, particularly for local-scaling diagnostics.

It is widely accepted (see e.g. Mason 1994) that LES has the potential to give us new information of reasonable, though not absolute, reliability, especially when the theoretical framework is reasonably settled. But the formulation, parametrization, boundary conditions and analysis of such models inevitably reflect existing theories. Comparison with independent data is a basic scientific requirement to estimate the accuracy with which it represents the real atmosphere.

Conversely, advances in idealized modelling make possible a more critical assessment of empirical results. Indeed one reason for conducting new experiments is to resolve whether any disagreements between old experiments and recent models reflect poor experimental technique. For instance, the various laboratory studies of stably-stratified turbulence are vulnerable to Reynolds-number effects and other problems. Detailed turbulence measurements in the atmospheric SBL do therefore fill important gaps in our knowledge.

In summary, when compared with Brown *et al.*, the present results

- agree fairly well for turbulence amplitude as a function of R_i;
- suggest, as do other empirical results, that the model a_w^{-1} is slightly too low;
- agree broadly with the (moderate) deviations of $\mathcal{F}$ and ς_θ from the BW curves;
- agree broadly for correlation coefficient $r_{w\theta}$ as a function of R_i, though becoming closer to the non-backscatter results for $R_i \gtrsim 0.15$;
- show intermittency near the surface which is difficult to reproduce in LES.

The final item raises questions which current research models cannot answer with confidence, since it is not clear theoretically how model idealizations relate to observed intermittency. This issue illustrates the need for data comparison, even when a detailed turbulence model appears to perform well in its own terms.

Acknowledgement

I would like to acknowledge the helpful comments on this work of many colleagues at Cardington and Bracknell. The assistance and professionalism of the Cardington technical and balloon staff was of course essential to the experiment. Alan Lapworth and Phil Hopwood have been particularly tolerant of the author's foibles.

Appendix: instrument response

The main response-limiting factor in the present measurements is the Gill length constant, around 1m. That this is not too bad can be inferred from the 10-20m resolution in the Large Eddy Simulations mentioned in the text, for comparable boundary layers. It would be laborious to check spectra for every case. Here an exhaustive analysis is not attempted, but some rough estimates are checked against a few cases, in order to estimate how far response issues might compromise the experiment.

A simple indicator of instrument response comes from the ratio WTHT/WT of heat-fluxes computed with slow thermistors to fast PRTs. When the turbulence length-scales are small, the slow sensor should give a lower flux by a fraction related to the instrument response length-scale. Fig. A1 shows most points (85%) give a good fit to

$$\mathrm{WTHT/WT} = [1 + 5\mathrm{m}/l_m]^{-1}$$

with all the exceptions occurring at smallest mixing-length l_m. Thus the response scale for 'slow heat-flux' seems to translate into a mixing-length scale around 5m. Since from Panofsky in Workshop on Micromet., p.154, one infers $\lambda_w/l_m \sim 5$ for neutral conditions, this suggests a spectral peak wavelength λ_w around 25m, giving a response frequency around 0.3 Hz. This extremely rough argument is consistent with the response frequency of the slow thermistor, as found in laboratory calibration tests, which should be the limiting factor in determining WTHT response.

The typical mixing-length l_m ~5m here corresponds to a probe mounted at 12.5m in a neutral surface-layer. Standard arguments and measurements (Kaimal 1973) suggest that in an inertial range the fractional error in stresses or fluxes from an instrumental which filters on a length-scale l_f varies as $(l_f/l_m)^{4/3}$. If the combined Gill/PRT system responds ~30 times faster than the Gill/slow-thermistor system, then under this scaling a typical 50% loss from slow WTHT implies only a 1% loss from fast WT. This is based on a Gill response length of 1m, as compared to a thermistor response timescale of 3s, converted to a lengthscale of 30m by assuming advection at $10\mathrm{ms}^{-1}$. This is however complicated by (i) the Gill response correction applied during processing and (ii) the slower response when the Gill is not pointing into the wind.

Note also that in practice the criteria for useful accuracy in measuring the poorly-documented behaviour of turbulence aloft in stable boundary layers is less stringent than for e.g. the relatively well-documented neutral surface-layer. In particular, say 10% errors in l_m in the more stable range correspond to only small changes in R_i and therefore are less significant than in the neutral surface-layer.

There is scope for further analysis of the present spectra & cospectra, with comparison. Fig. A2 shows a temperature spectrum $nS_\theta(n)$ with a credible inertial subrange. Spot checks suggest that this is typical of the moderately stable cases at least. One point in Run E3 was identified as anomalous from the temperature variance profile and $nS_\theta(n)$ was found to increase steadily with wavenumber as if dominated by high-frequency noise, giving spuriously high σ_θ. As mentioned in the main text, electronic problems are believed to be responsible. In non-dimensional diagnostics involving σ_θ such as the correlation coefficient this point was found on re-examination to be an

outlier whose removal would 'improve' the scatter-plot, but did not significantly affect interpretation.

Fig. A3 shows a co-spectrum from the second-lowest probe in run E1, which seems consistent with a negligible loss by finite instrument response. This was at height 60m, with $R_i \sim 0.15$ and $l_m \simeq 9$m. Kaimal (1973) measured turbulence spectra in the stable surface-layer. His stability scaling (lengthscales $\sim z/R_i$) was doubtful both at the neutral and the stable end and he quotes it only for $0.05 < R_i < 0.2$. In his Fig. 3 the only point at higher R_i deviates from his scaling in a manner consistent with $R_{ic} = 0.25$. Further combining that figure with the spectra suggests $(\lambda_m)_w \sim L$, where L is the Monin-Obukhov length. Typically in the more stable regime $L \sim 10 l_m$. Kaimal introduces variable standard spectral frequencies f_0 which are different for different variables. In fact $(f_0)_w \sim z/3(\lambda_m)_w$ whilst $(f_0)_{w\theta} \sim 1.5z/(\lambda_m)_{w\theta}$. Since he finds $(f_0)_{w\theta} \sim 2(f_0)_w$ this implies $(\lambda_m)_{w\theta} \sim 2.5(\lambda_m)_w$. His results also imply that the spectral peak wavelength $(\lambda_m)_\theta/(\lambda_m)_w \sim 3.3$. For a sharp spectral filter λ_f the proportion of flux lost $\sim 2(\lambda_f/(\lambda_m)_{w\theta})^{4/3}$.

The probe mentioned shows $(\lambda_m)_{w\theta} \sim 250$m, $(\lambda_m)_\theta \sim 200$m and $(\lambda_m)_w \sim 100$m for a mixing-length of 10m. The ratio $(\lambda_m)_w/l_m$ is similar to those implied from Kaimal's data, and the ratios between the length-scales are not far out, given the uncertainty in estimating a peak. However he quotes $(\lambda_m)_w/z \sim 0.093/R_i$ implying $(\lambda_m)_w \sim 40$m, lower than observed by a factor 0.4, whilst the 'Kaimal' prediction for $(\lambda_m)_\theta$ is 60% of observed. Close agreement was not expected theoretically for the lengths, given the difference between surface-layer and boundary measurements, but the broad agreement between ratios suggests that using local scaling the two may be roughly comparable. In terms of mixing-length dependence on R_i as plotted in Fig. 9a, this point is fairly representative but the Kaimal prediction lies within the data scatter.

A rough estimate from the probe-sonic intercomparison of Grant (1992) suggested a response scale l_r of 0.5m by fitting a standard power spectral lagged-response function

$$[1 + (2\pi l_r/\lambda)^2]^{-1}$$

where as usual λ is the wavelength. This gives a spectral response of about 60% at wavelength 4m and 30% at 2m, implying a loss of only around 1% in $\overline{w'\theta'}$ and 3% in σ_w^2 for the above case.

Admittedly the single comparison for $\overline{wT}$ shows a 20% loss from the probe, although this comparison is inherently limited without corrections to sonic temperature. Furthermore the cospectrum for uw also differs more than the above arguments suggest. We have ignored the effects of phase shifts which tend to contaminate the cospectrum with the quadspectrum. These shifts are first-order in l_r whereas the change in the spectral response function (which ignores phase information) is second-order. But analysis showed that the quadspectrum $Q_{w\theta}$ fluctuated in sign, and at small scales was much smaller than the cospectrum, leading to uncertainties of less than 1% in the total.

Given all the uncertainties about SBL turbulence, the response of the turbulence instrumentation as presently deployed is adequate to the present problem, and the reliable measurement of R_i is probably the greater challenge.

References

Belcher, S.E. and Wood, N. (1994): The form and wave drag due to stably stratified flow over low hills. Submitted to QJRMS.

Brost, R.A. and Wyngaard, J.C. (1978): A model study of the stably-stratified planetary boundary layer. *J. Atm. Sci.* , **35** 1427-40.

Brown, A.R., Derbyshire, S.H. and Mason, P.J. (1994): Large eddy simulation of the stable atmospheric boundary layer with a revised, stochastic subgrid model. To appear in *Quart. J. Roy. Met. Soc.*

Caughey, S.J., Wyngaard, J.C. and Kaimal, J.C. (1979): Turbulence in the evolving stable boundary layer. *J. Atm. Sci.* **6**, 1041-1052.

Derbyshire, S.H. (1990): Nieuwstadt's stable boundary layer revisited. *Quart. J. Roy. Met. Soc.*, **116**, 127-158.

Derbyshire, S.H. (1994): Observed stable boundary layers compared with idealized models. 'Accepted in principle' by *Bound. Layer Meteor.*

Derbyshire, S.H. and Wood, N. (1994): The sensitivity of stable boundary layers to small slopes and other influences. *Proc. 4th IMA Conf. Waves and Stably-Stratified Turbulence*, ed. N.Rockliff and I.P.Castro.

Dharssi, I., Lorenc, A., and Ingleby, N.B. (1992): Treatment of gross errors using maximum probability theory. *Quart. J. Roy. Meteor. Soc.*, **118**, 1017–1036.

Grant, A.L.M. (1992): A comparison between the Cardington turbulence probe and a sonic anemometer. Cardington Technical Note 13.

Grant, A.L.M. (1994): Wind profiles in the stable boundary layer, and the effect of low relief. *Quart. J. Roy. Meteor. Soc.*, **120**, 27–46.

Kaimal, J.C. (1973): Turbulence spectra, length scales and structure parameters in the stable surface layer. *Bound. Layer Meteor.*, **4**, 289–309.

Lapworth, A.J. and Mason, P.J. (1988): The new Cardington balloon-borne turbulence probe system. *J. Atmos. Oceanic Technol.* **5**, 699-714.

Mahrt, L. (1988): Turbulence in stratified flow. Proc. AMS Conf. San Diego, 1988, 131-135.

Mason, P.J. (1994): Large-eddy simulation: A critical review of the technique. *Quart. J. Roy. Meteor. Soc.*, **120**, 1–26.

Mason, P.J. and Derbyshire, S.H. (1990): Large Eddy Simulation of the Stably-Stratified Atmospheric Boundary Layer. *Bound. Layer Meteor.*, **53**, 117–162.

Figure 1: Profile compilation for

010293: Anticyclone over North Sea giving light SE'lies. Sunny afternoon, cloudless by dusk. Slightly misty by end of flying. Low-level jet develops and breaks down as boundary layer deepens. Little turbulence above 100m. Substantial veer with time at all levels, but also 'normal' 40° veer with height by end of flying. Net IR about 55 Wm^{-2} upwards. Sunset 16:49.

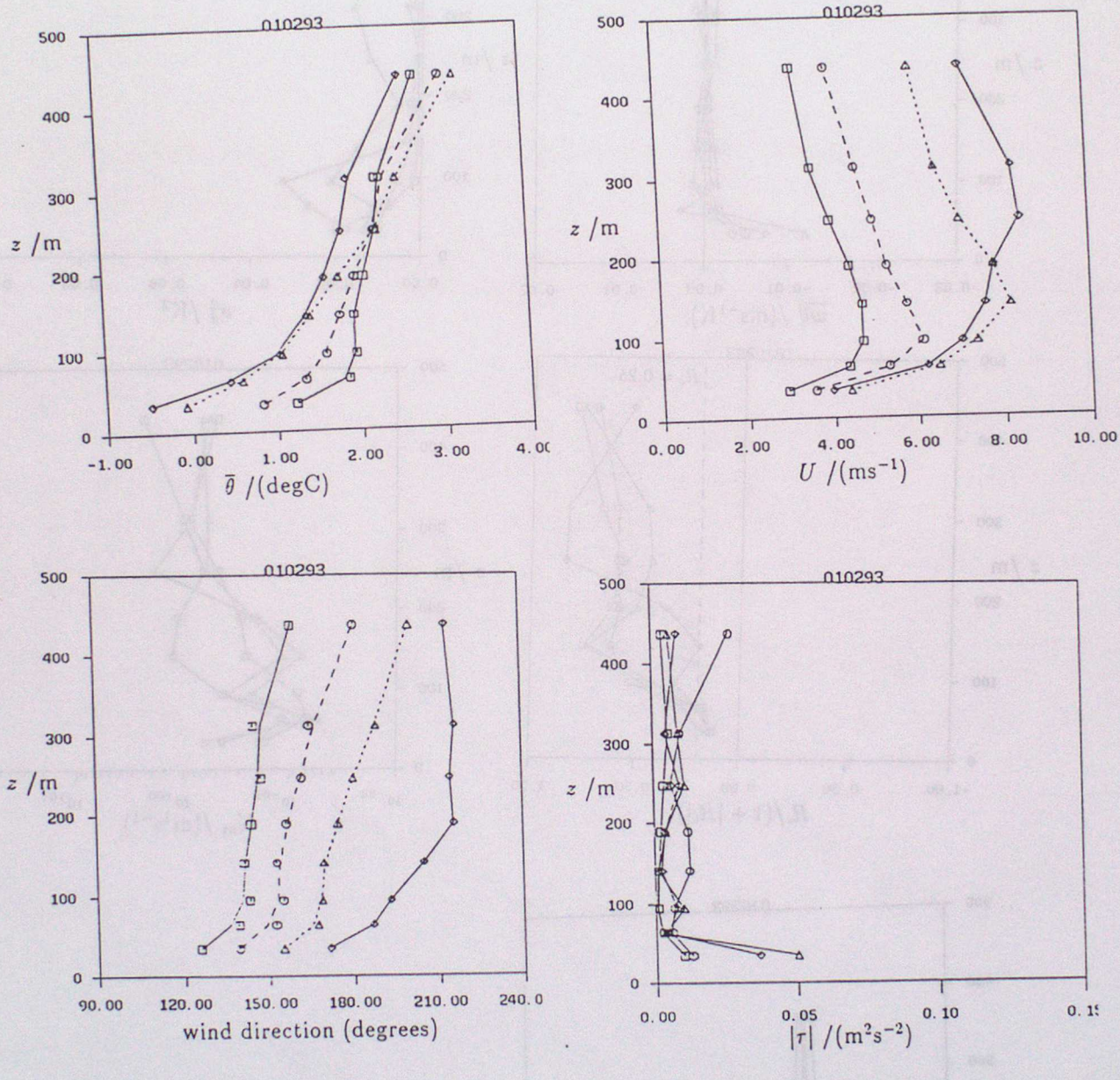

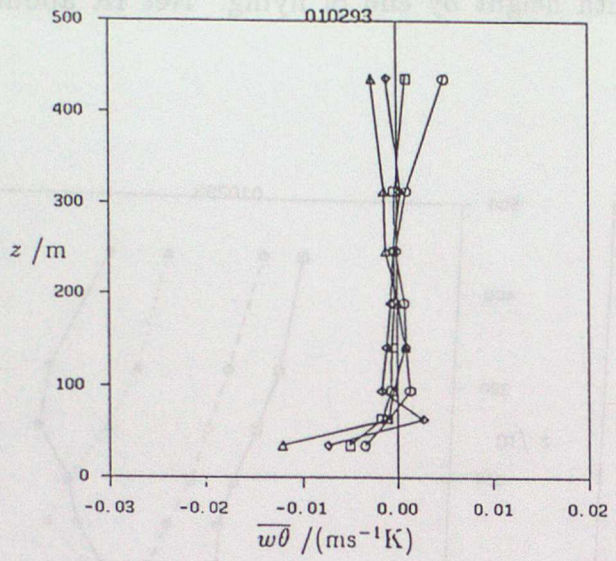

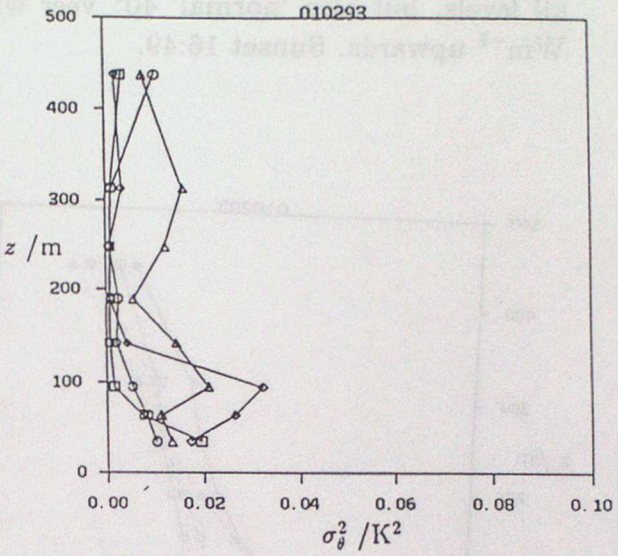

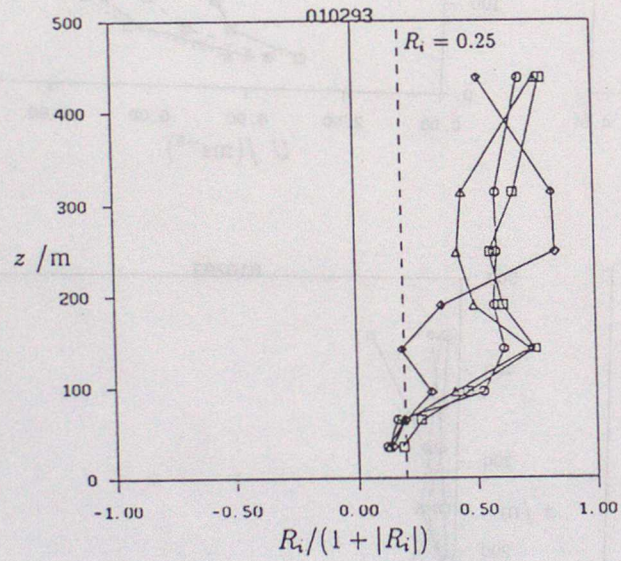

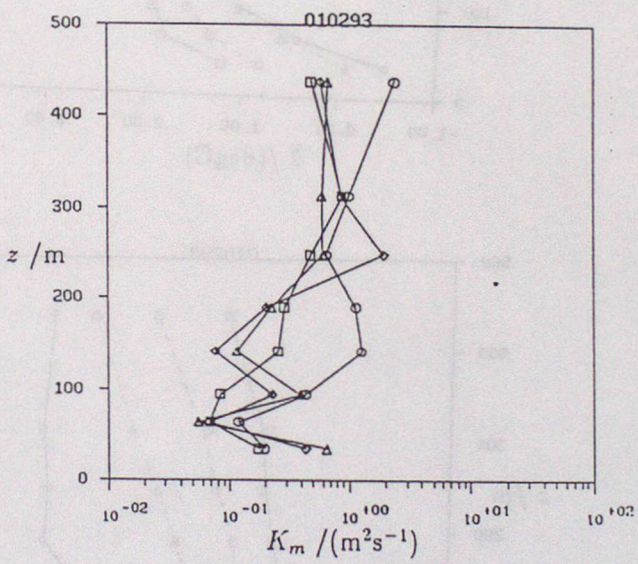

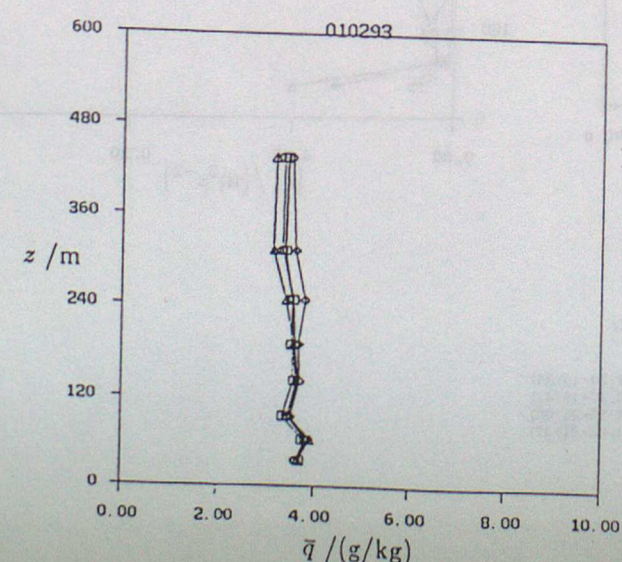

PLOTTING KEY

RUN F (17:24-18:34)
RUN G (18:37-19:47)
RUN H (19:50-21:00)
RUN I (21:02-21:37)

Figure 3: Profile compilation for
090393: Similar to 080393, but winds lighter. Strong wind veer with time, but developing 'normal' boundary layer veer (much as on 010293). Turbulence dying away above about 100m ($|\tau|$ from top probe on run F suspect). Some problems with the slow temperature signal on probe iii (effectively ignored by smoother). Sunset 17:56.

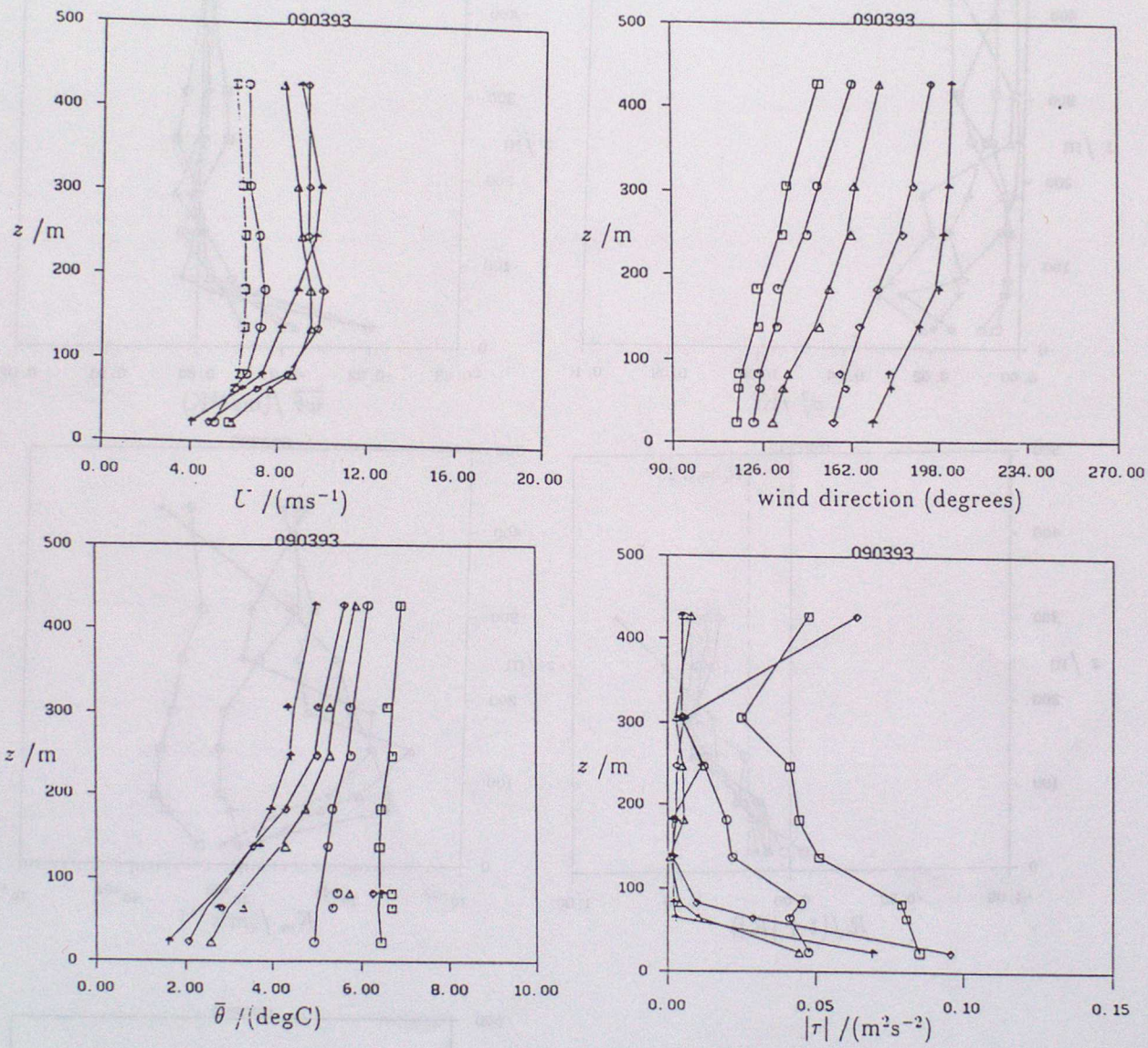

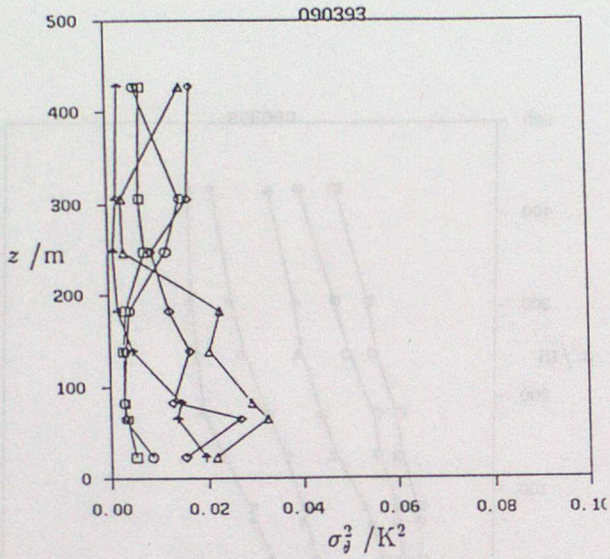

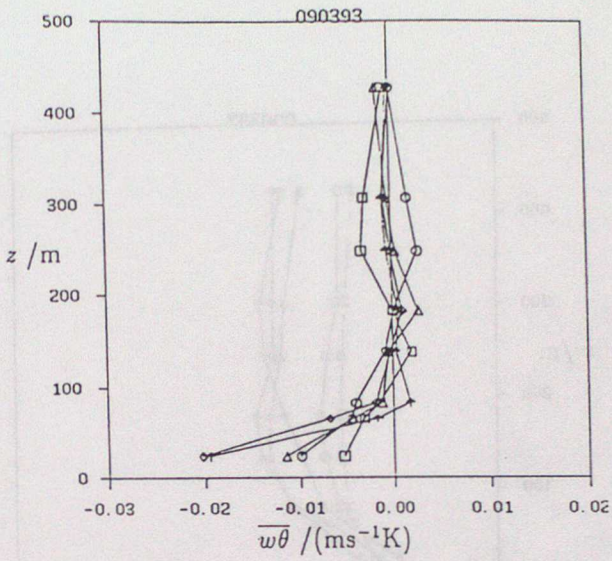

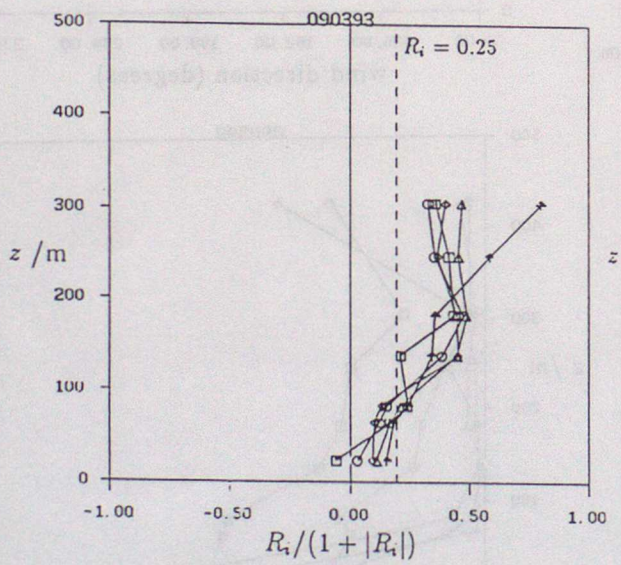

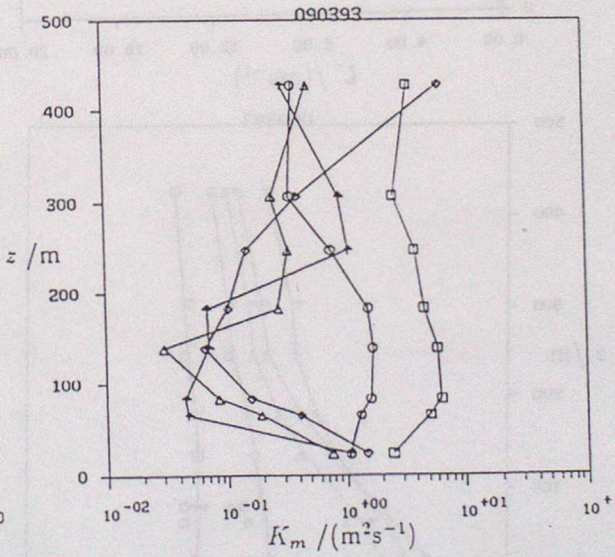

PLOTTING KEY

- □ RUN B (16:00-17:10)
- ○ RUN C (17:14-18:24)
- △ RUN E (18:45-19:55)
- ◇ RUN F (19:55-21:05)
- ▲ RUN G (21:06-21:42)

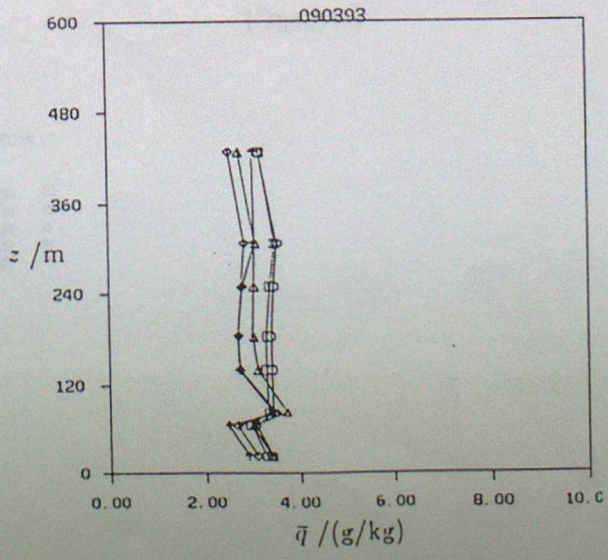

Figure 2: Profile compilation for
080393: Anticyclone over Scandinavia feeding dry, moderate SE'lies over area. Sunny, pleasant afternoon with low relative humidities. Little or no cloud, apart from trace of cirrus. Net IR about 60 Wm^{-2} upwards. With reasonably strong winds aloft, and substantial surface cooling, this case resembles idealized models, with a nocturnal jet, 40° veer developing across the boundary layer, flux profiles 'reasonable' in model terms, and R_i close to 0.25. Sunset 17:54.

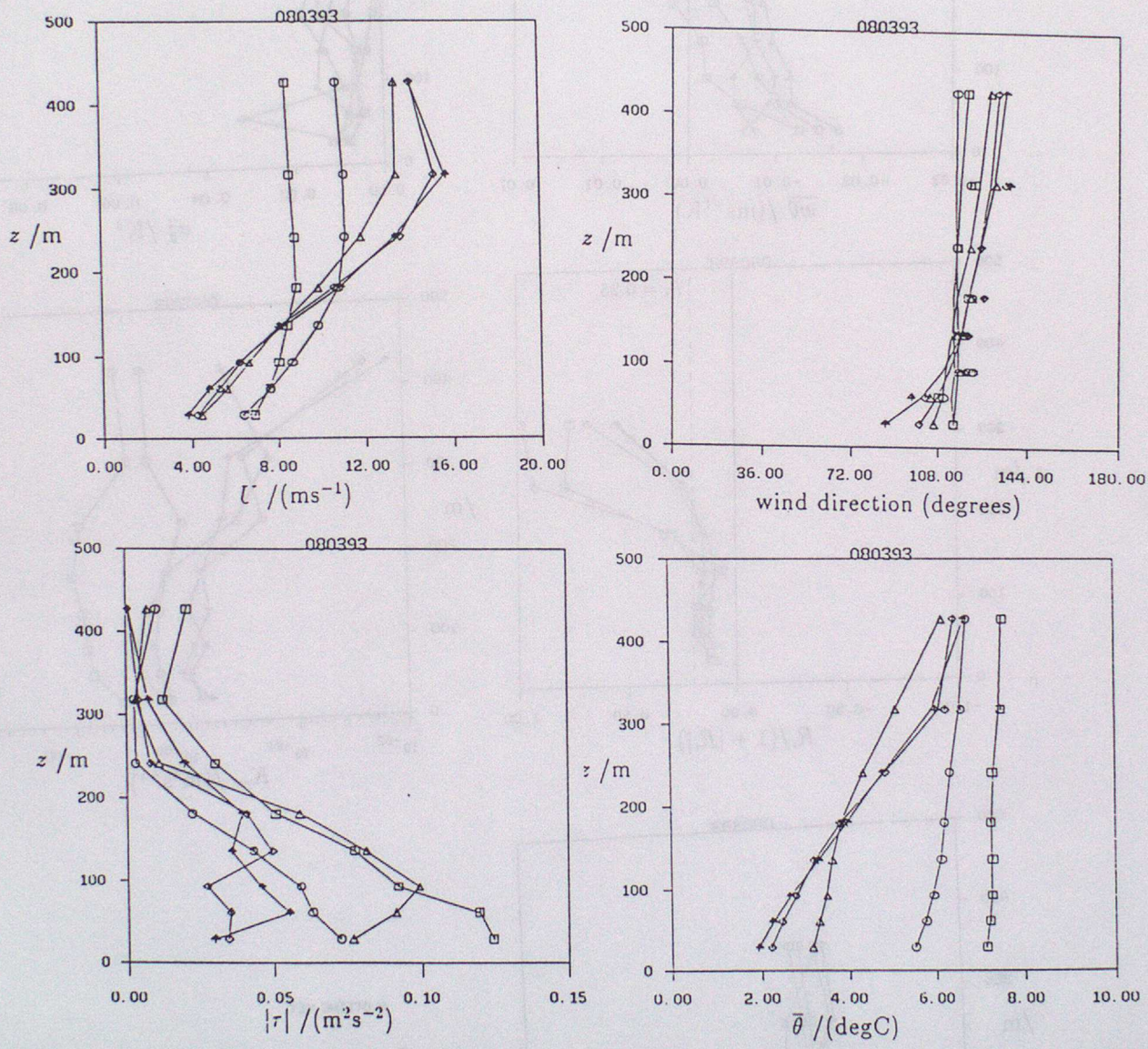

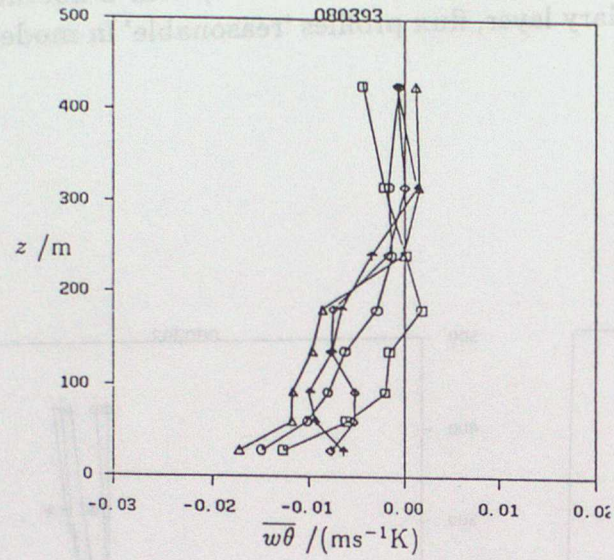

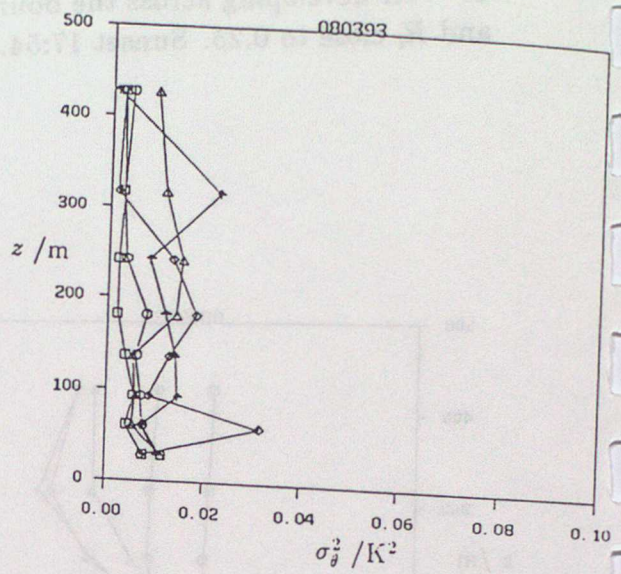

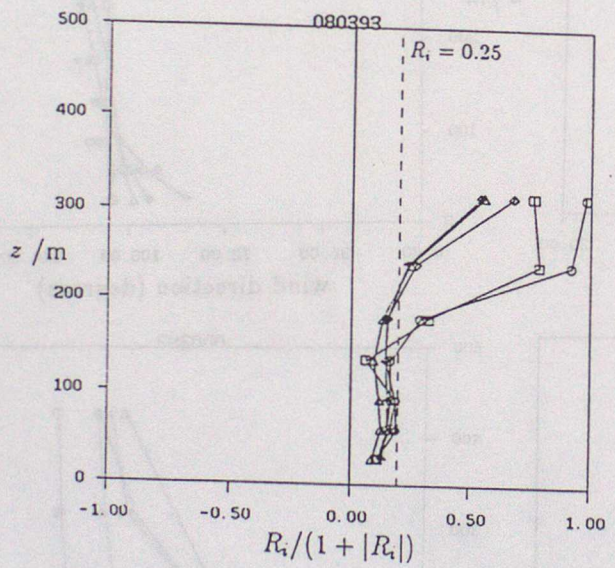

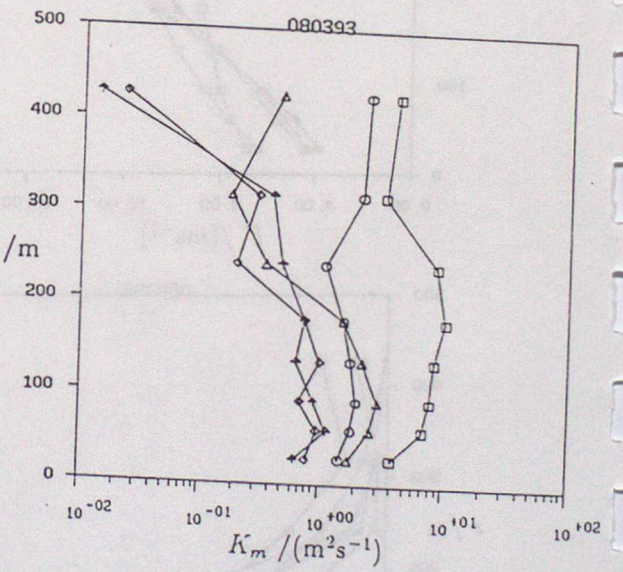

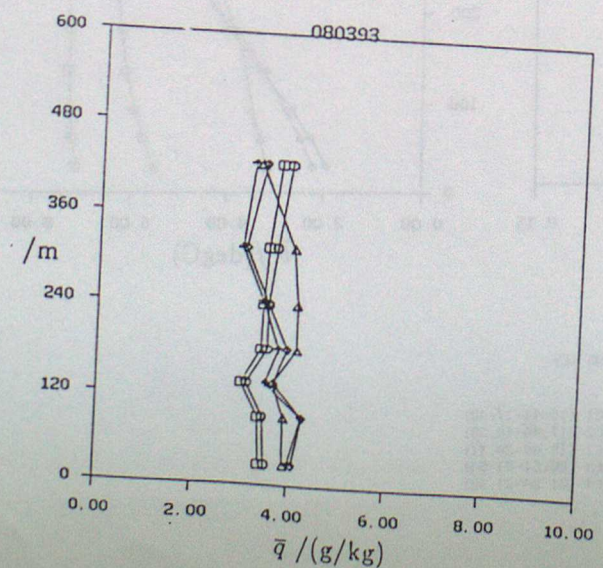

PLOTTING KEY

- RUN C1 (16:41-17:40)
- RUN C2 (17:48-18:55)
- RUN E1 (19:44-20:17)
- RUN E3 (20:51-21:54)
- RUN E4 (21:24-21:58)

Figure 4: Profile compilation for
101093: Moderate SW'ly flow between high over E.Europe and Atlantic low. 8/8 Sc at around 4000′ throughout flying period. Shows the normal SBL 'signals' in wind-direction etc. but rather weakly, and with little turbulence. Net IR below $10 \mathrm{Wm}^{-2}$ upwards. Sunset 17:58.

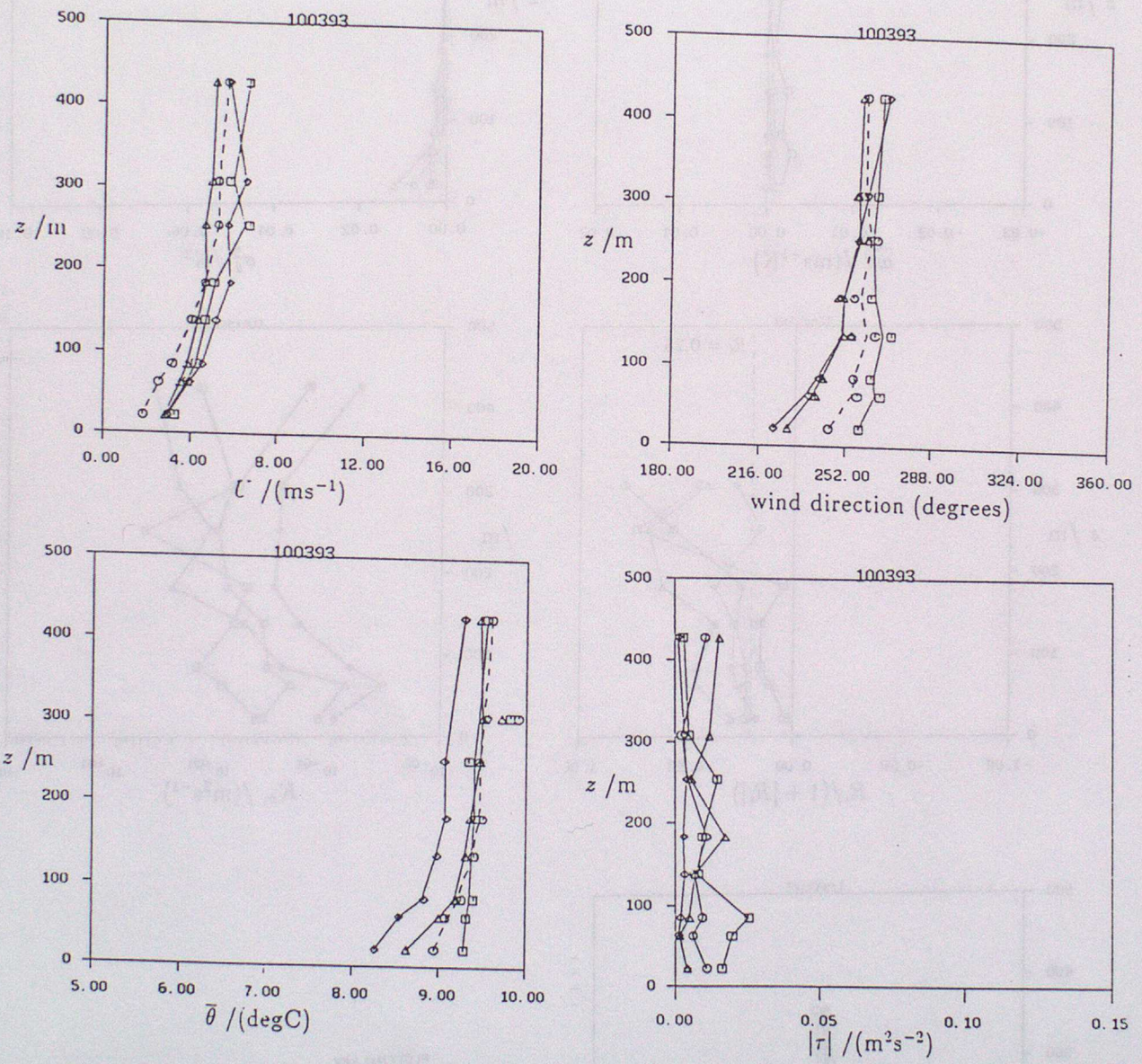

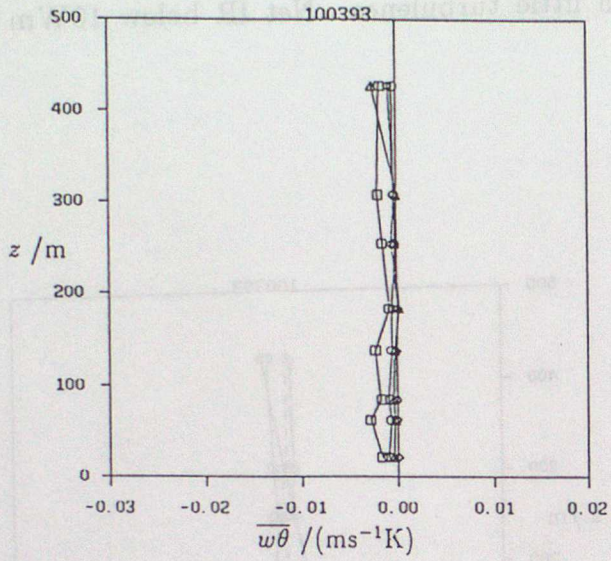

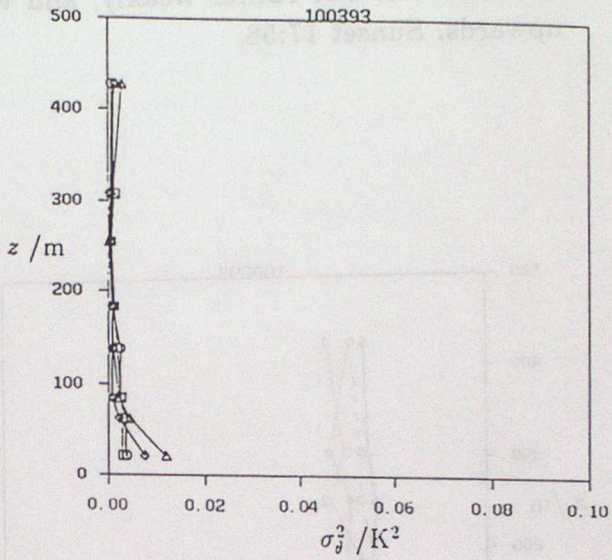

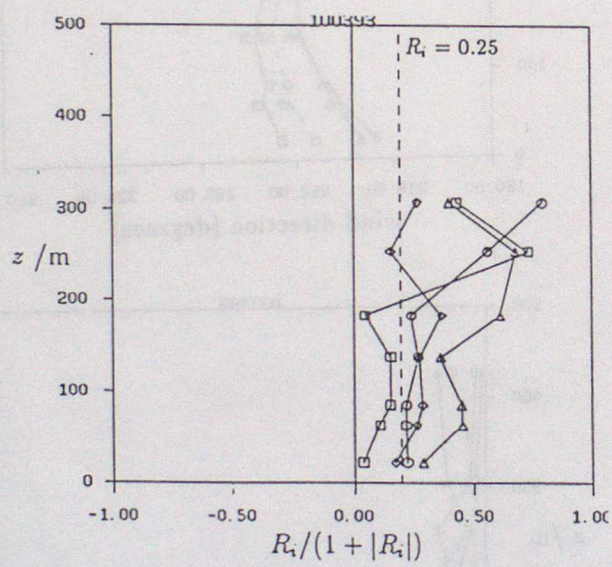

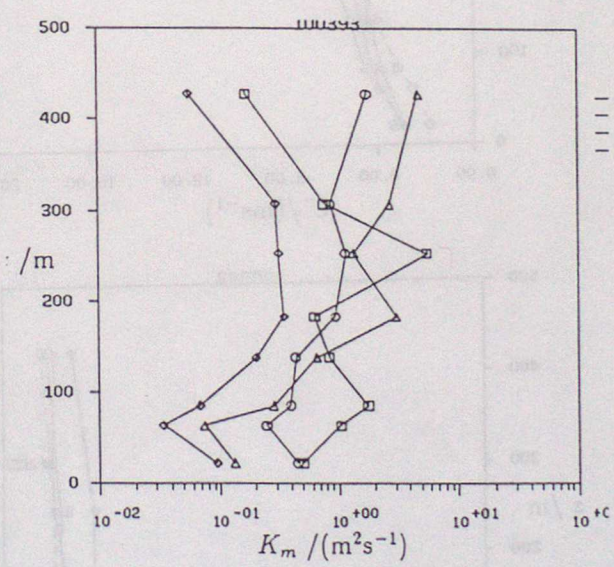

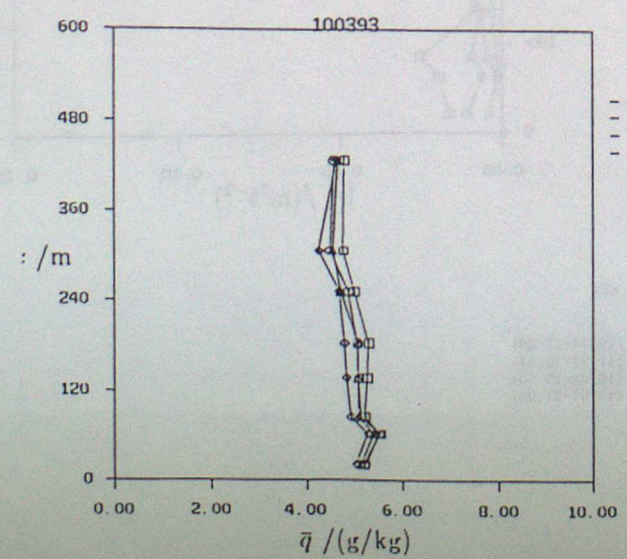

PLOTTING KEY

RUN B (16:14-17:24)
RUN C (17:27-18:37)
RUN D (18:40-19:50)
RUN E (19:51-21:00)

Figure 5: Profile compilation for
110393: Light-moderate S'ly. Only high cloud (about 3/8 Ci) reported. Quite large net IR (around $50 \mathrm{Wm}^{-2}$), and some relatively large near-surface upward sensible heat-fluxes. Final run shows little turbulence above 100m. Sunset 18:00.

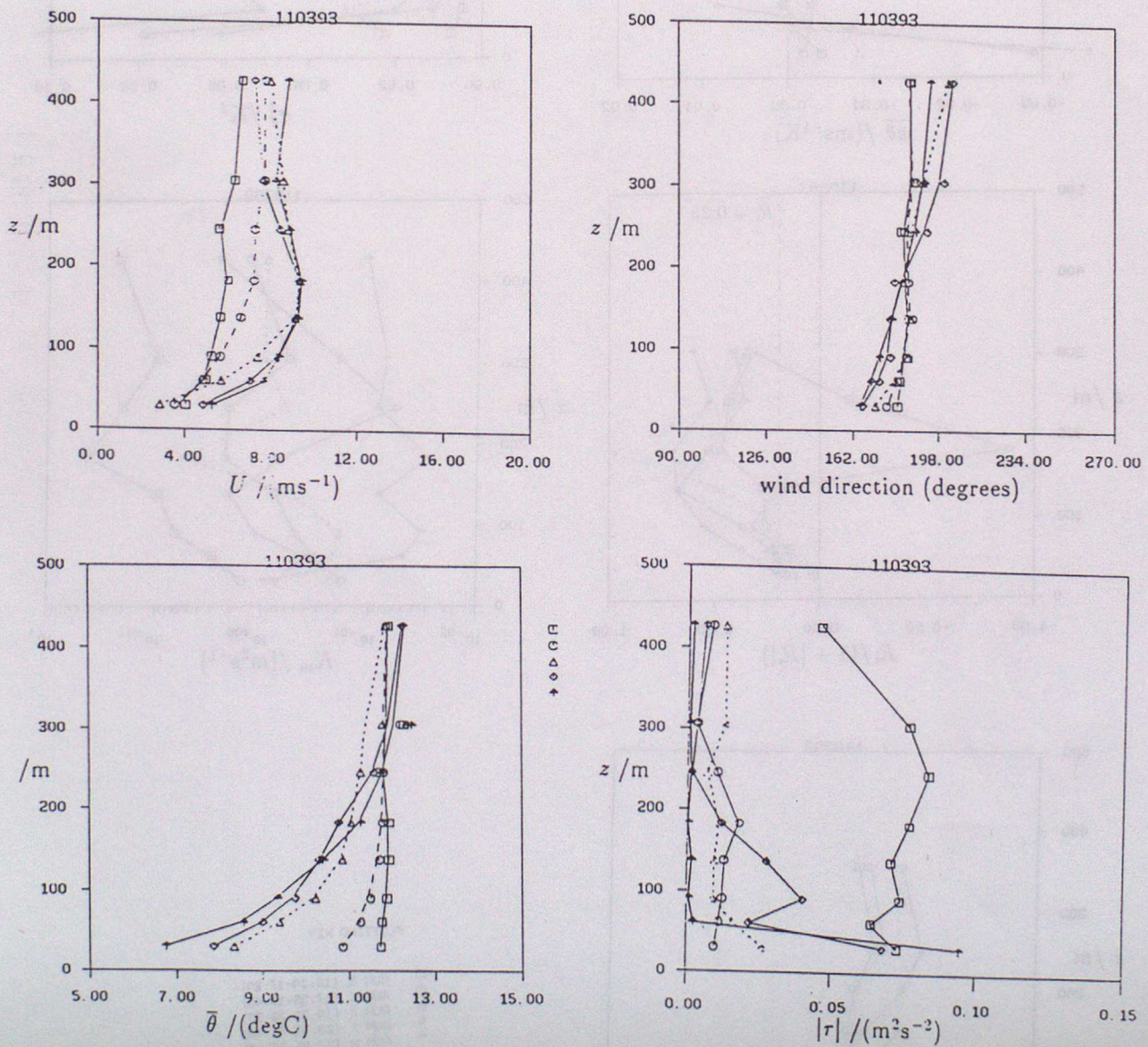

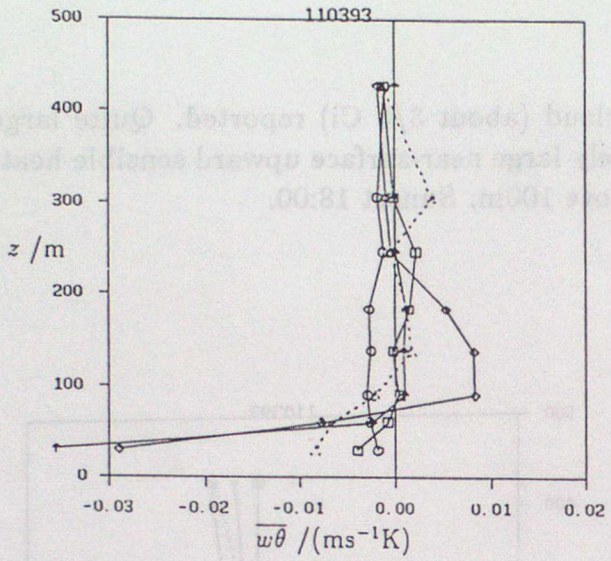

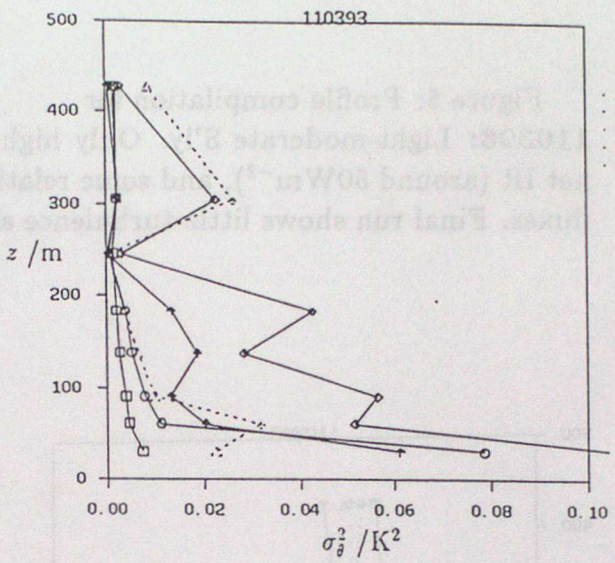

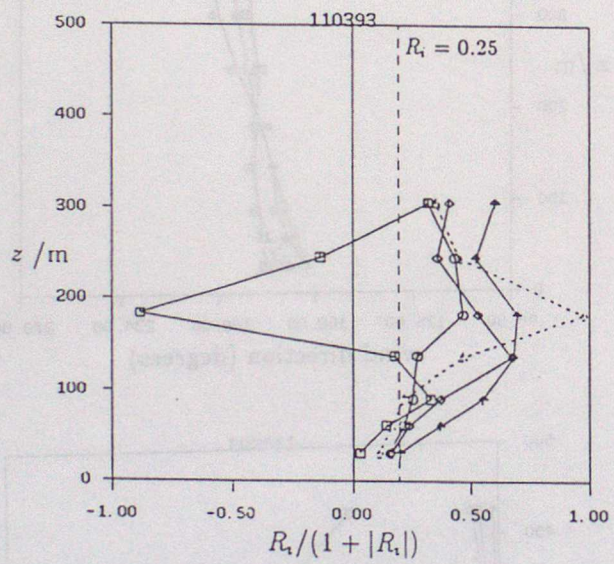

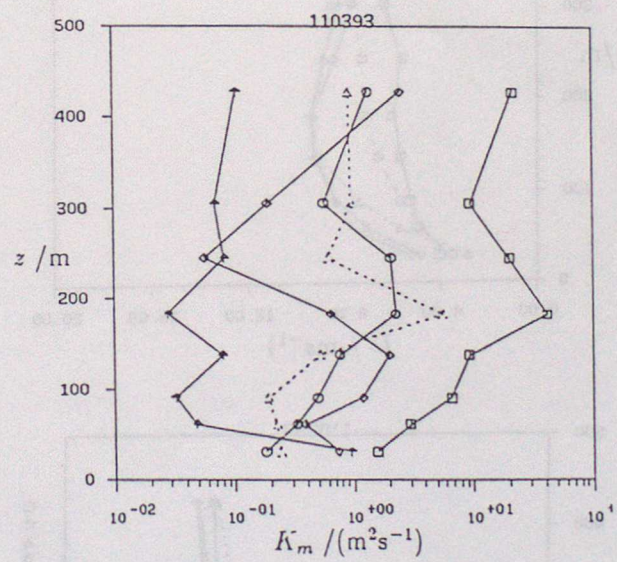

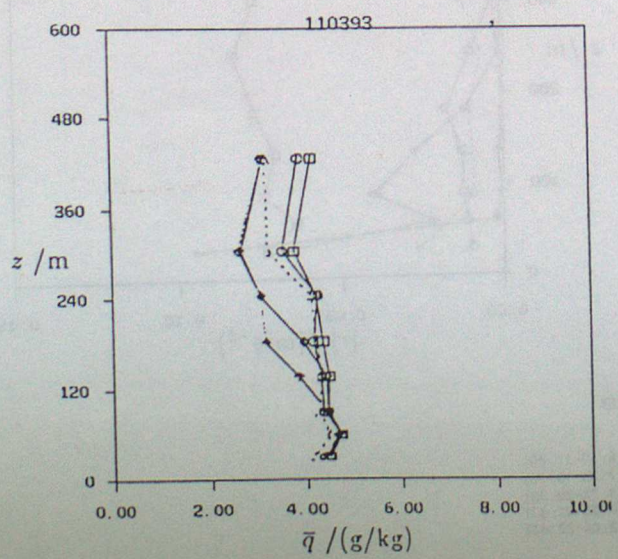

PLOTTING KEY

RUN B (16:19-17:29)
RUN C (17:35-18:45)
RUN E (19:22-20:33)
RUN F (20:33-21:43)
RUN H (22:05-22:43)

Figure 6: Profile compilation for
190393: Light-moderate anticyclonic W'ly. Afternoon 1/8 Sc, gone by 19:00. θ-profile suggests SBL developing about 250m deep, but turbulence profiles (and R_i) suggest more like 100m. Net IR about 60 Wm^{-2} upwards. Two probes show significant temperature offsets, detected and corrected by intercomparison. Sunset 18:13.

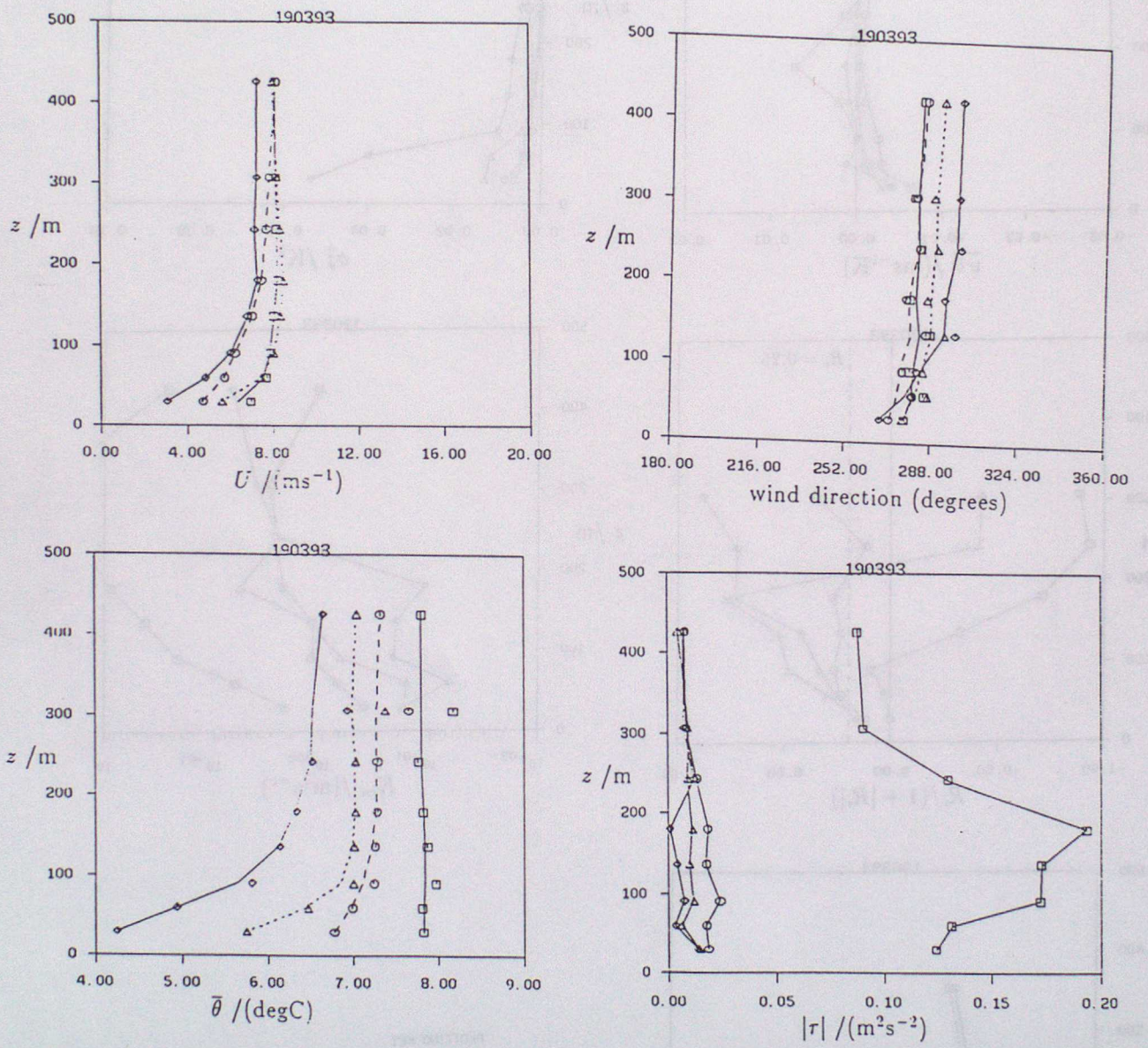

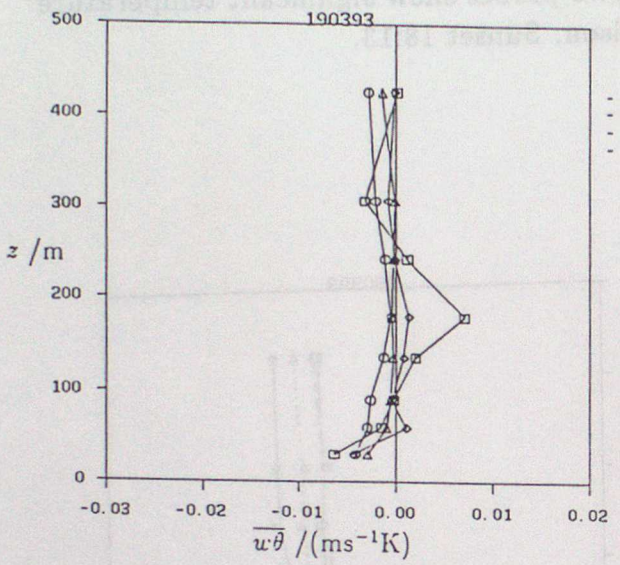

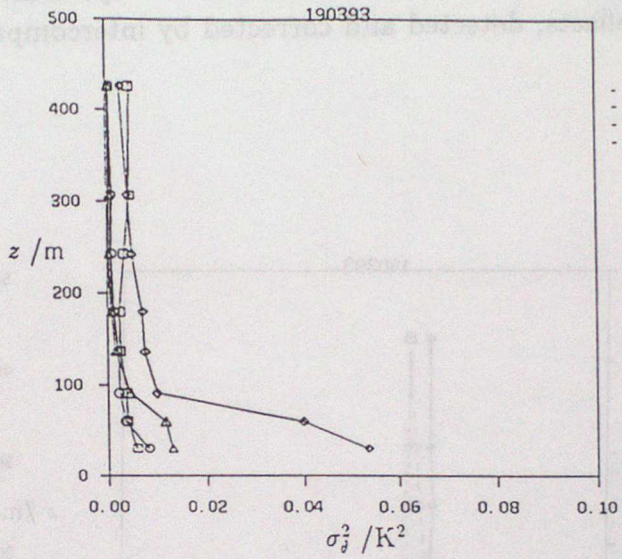

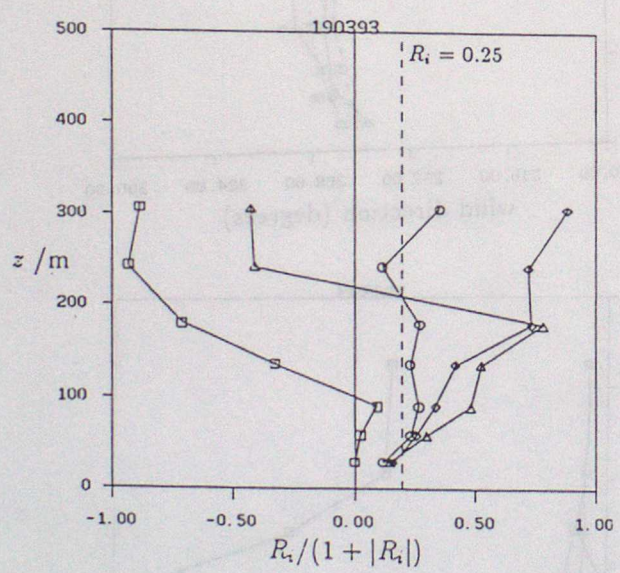

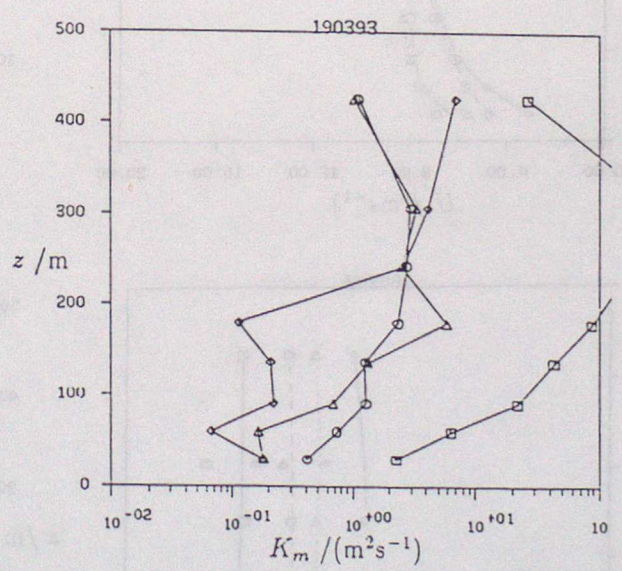

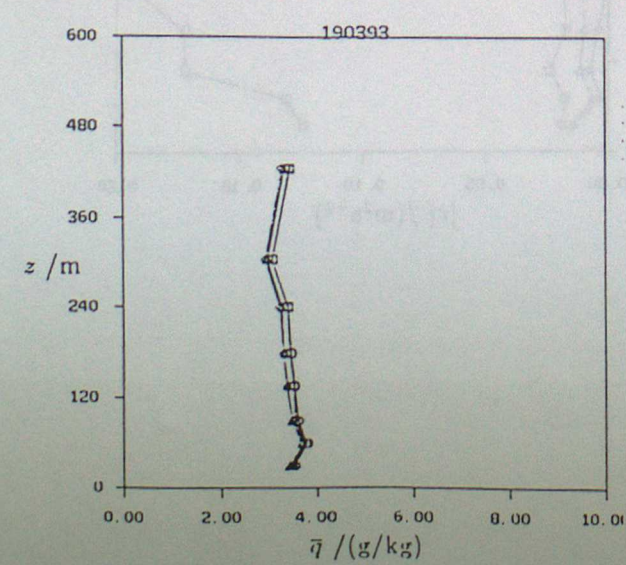

PLOTTING KEY

◇ △ ○ □

RUN B (16:30-17:40)
RUN C (17:45-18:55)
RUN E (19:15-20:25)
RUN F (20:30-21:40)

Figure 7: Profile compilation for
260393: Light anticylonic E'ly. Partial cloud-cover (3/8 Cu/Sc) at start of flying period, gone by 19:00. Shallow (< 100m) and strong ground-based inversion developing, with very little turbulence above. Net IR about 65 Wm^{-2} upwards. This was the only night with evidence for wind *backing* with height in the boundary layer, and seems roughly consistent with a tendency for drainage from the SW. Noticeable temperature offsets on two probes, as on 190393 (the same probes in fact). Sunset 18:25.

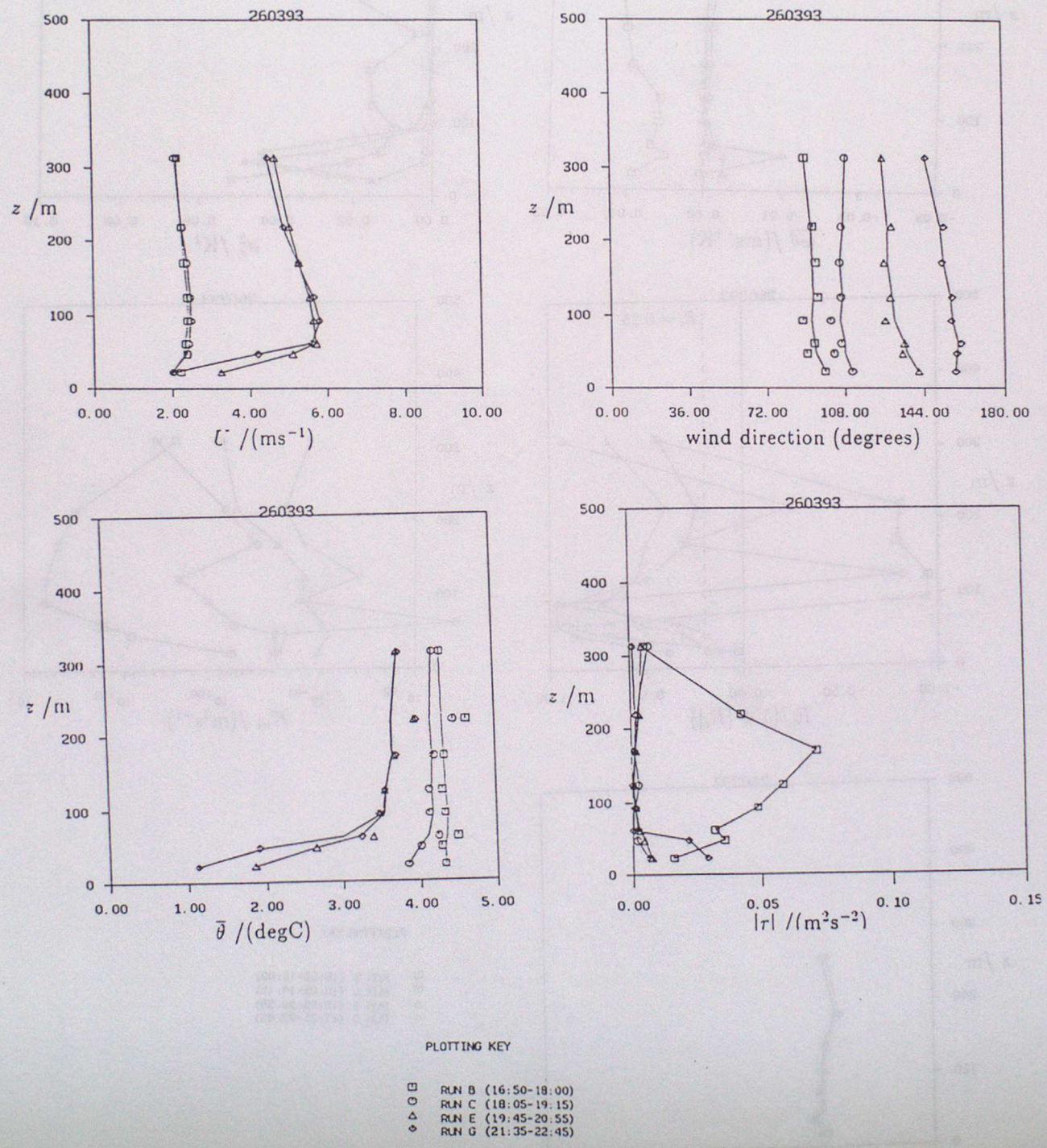

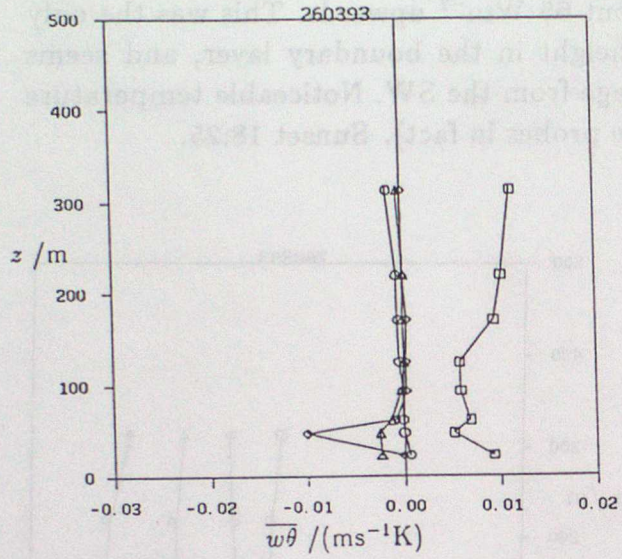

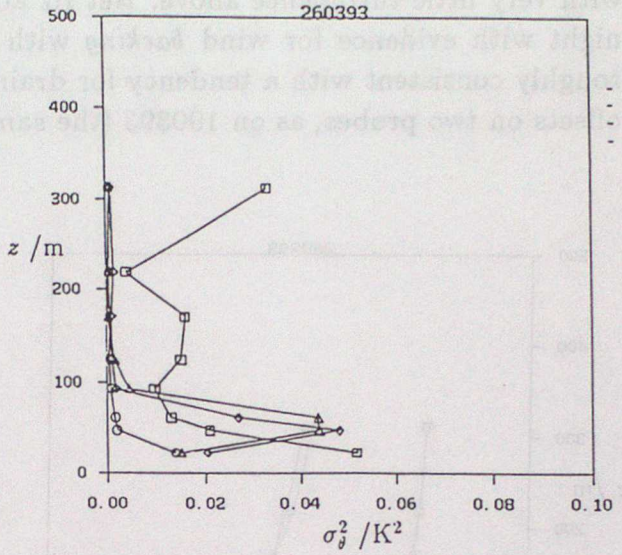

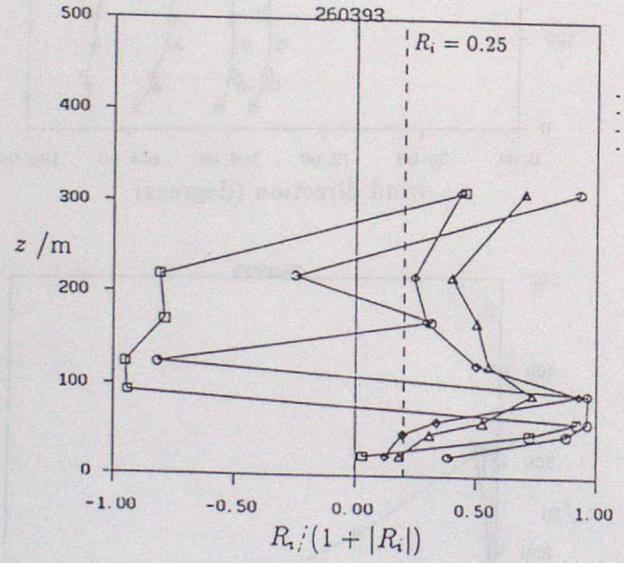

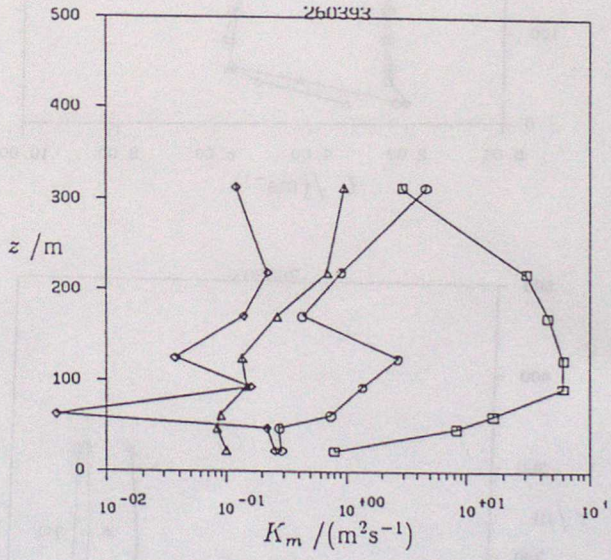

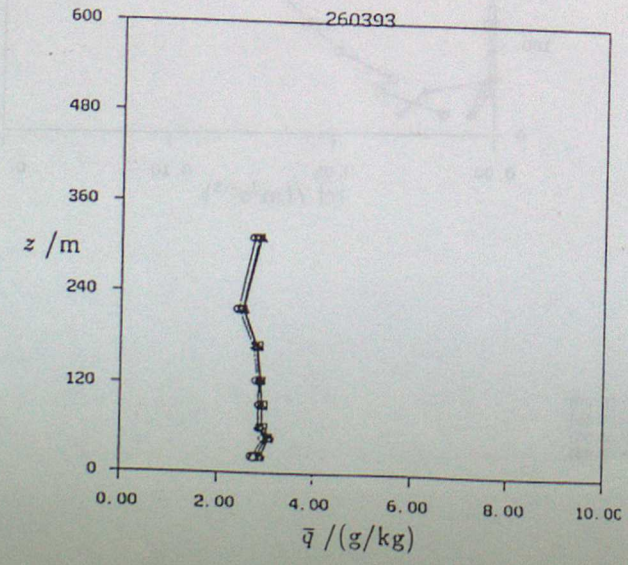

PLOTTING KEY

- RUN B (16:50-18:00)
- RUN C (18:05-19:15)
- RUN E (19:45-20:55)
- RUN G (21:35-22:45)

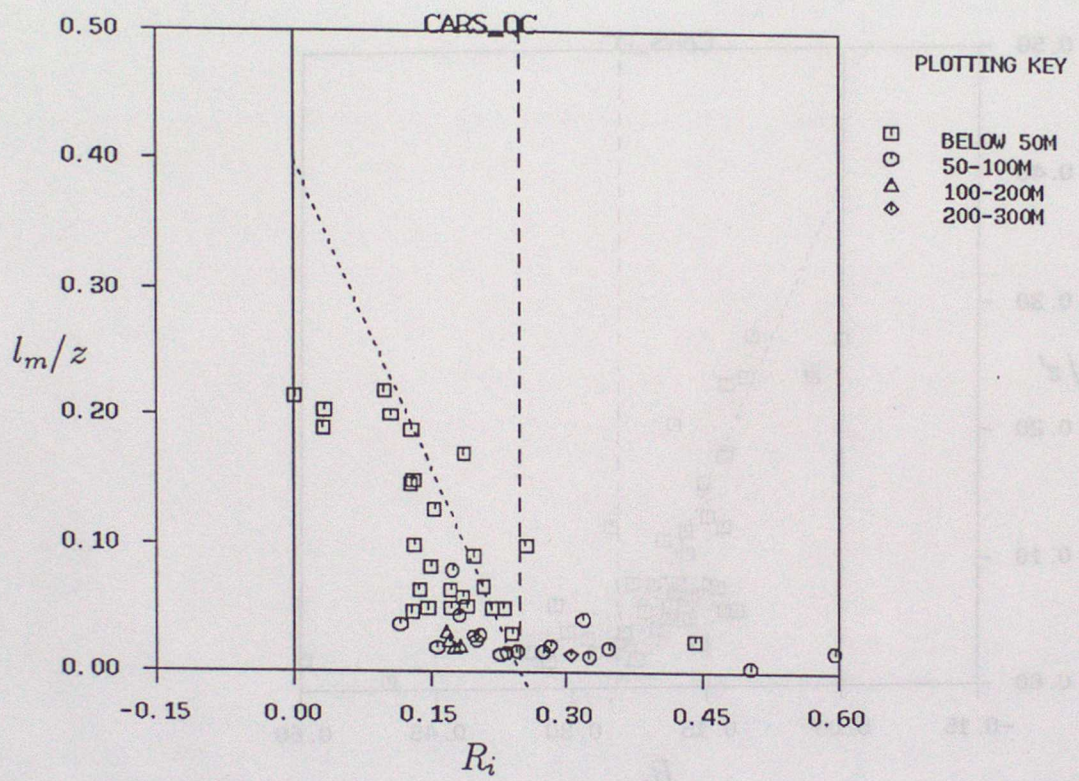

Figure 8a: Mixing-length l_m nondimensionalized by height z against R_i for quality-controlled data (rejected shears $< 0.04\text{s}^{-1}$). Dotted line is not a formal best fit but the simplest linear interpolation between standard values at $R_i = 0$ and $R_i = 0.25$.

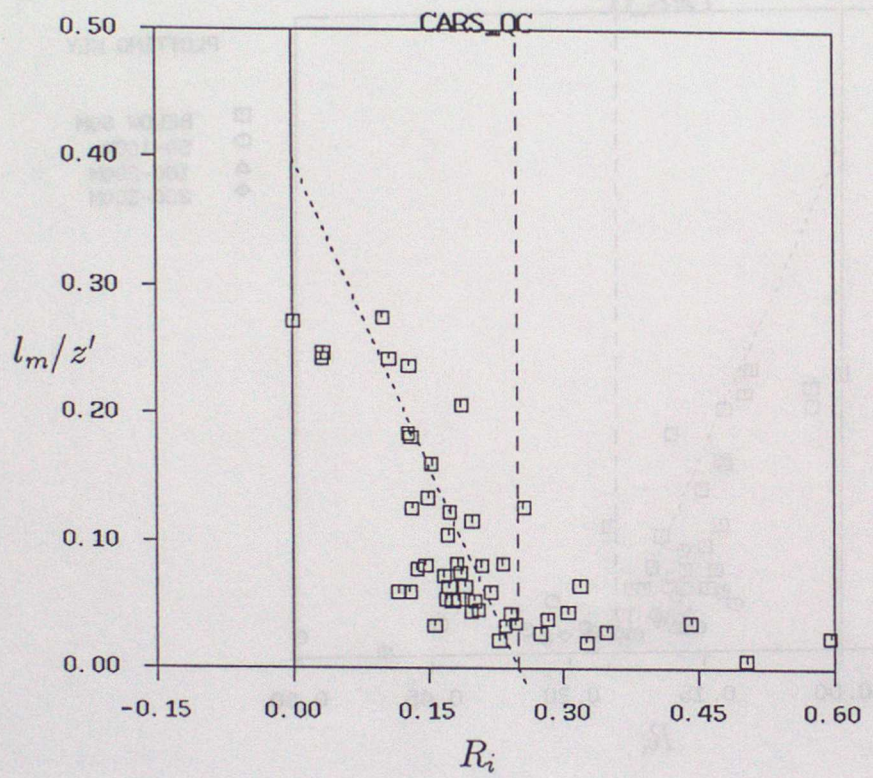

Figure 8b: As 8a, but with mixing-length nondimensionalized by z', as described in the text.

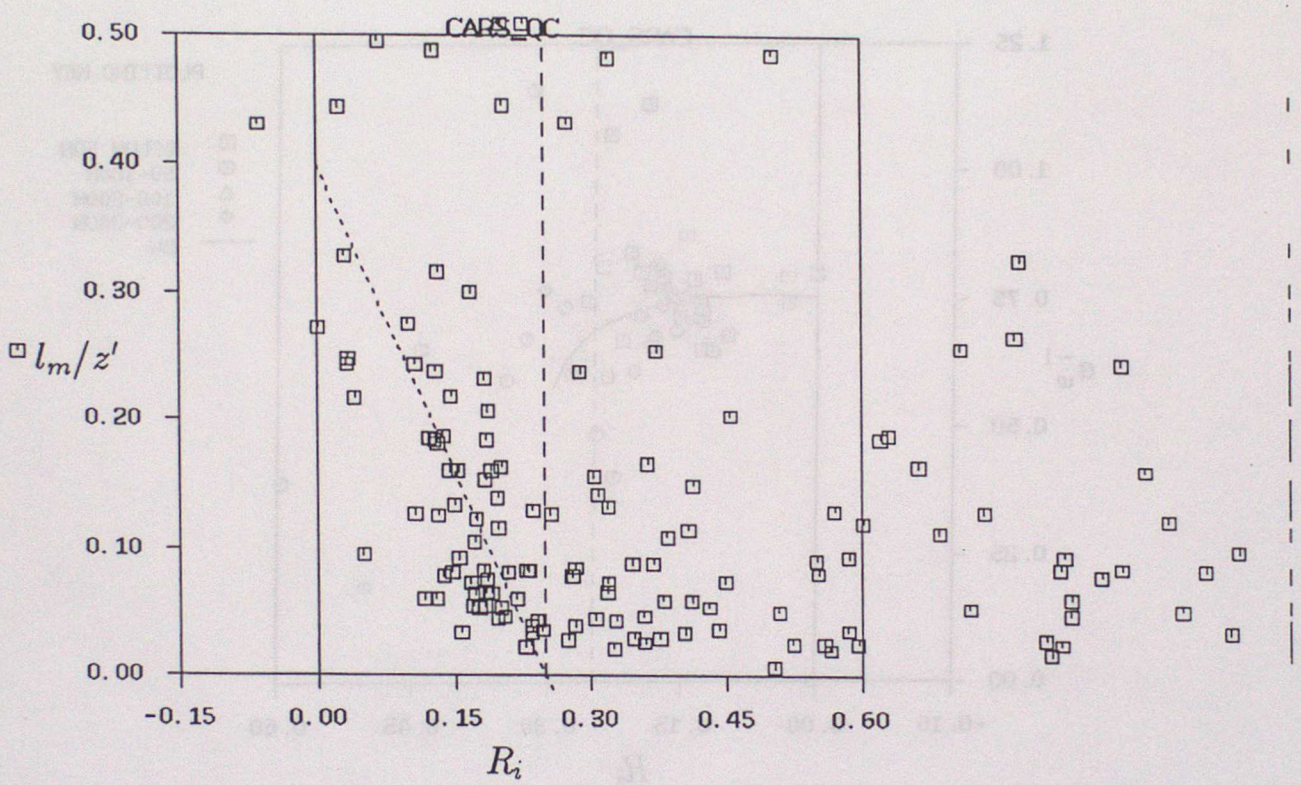

Figure 8c: As 8b, but removing all quality-control. Note the great scatter with many points offscale, and the potential for biasing results primarily through inaccurate measurement of R_i.

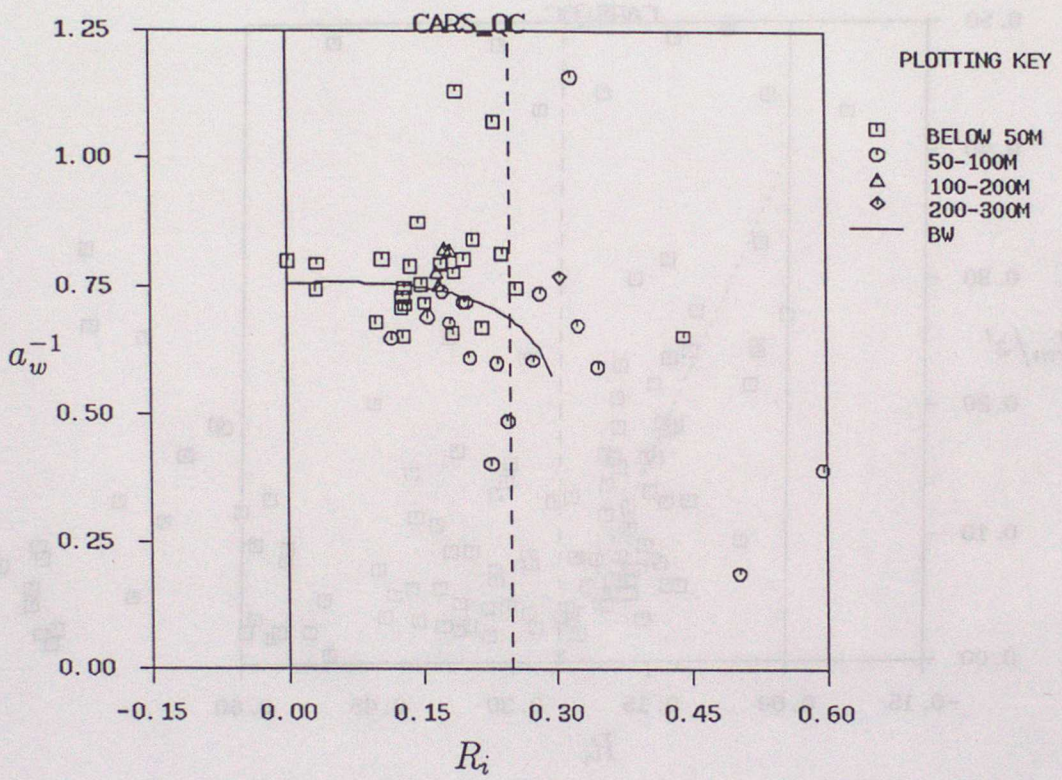

Figure 9a: $a_w^{-1} = |\tau|^{1/2}/\sigma_w$ against R_i, quality-controlled as in 8a.

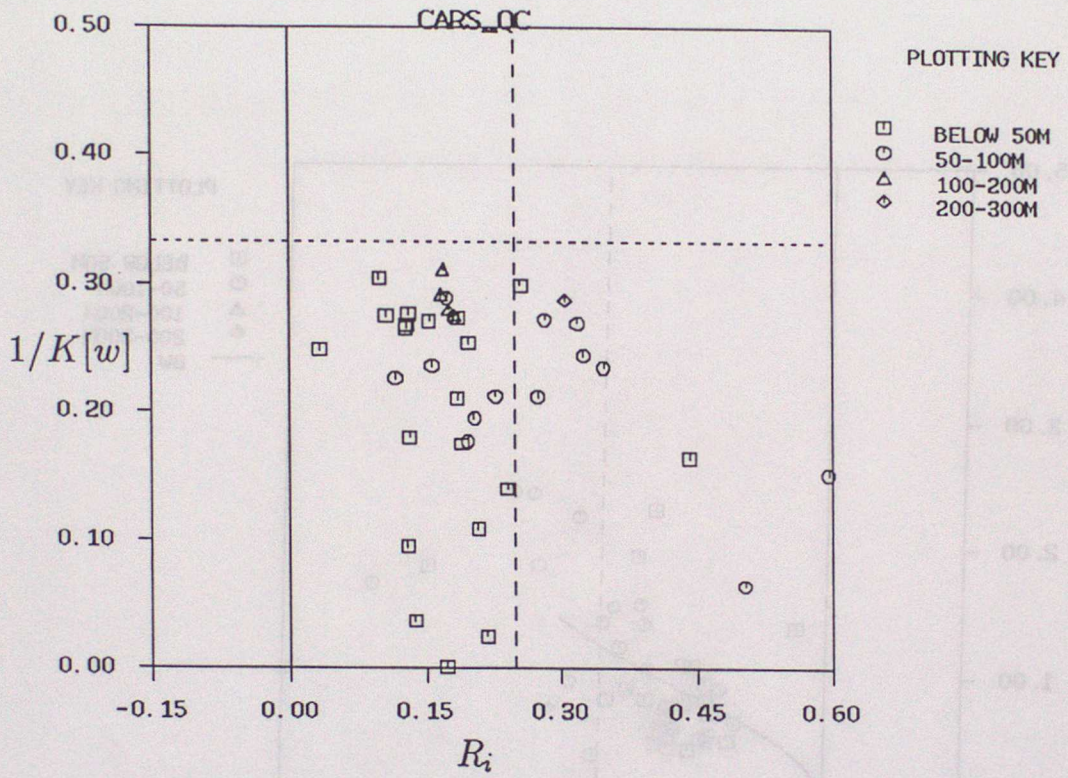

Figure 9b: $1/K[w]$, reciprocal kurtosis of vertical velocity (see text), against R_i. A horizontal dashed line shows for comparison the Gaussian expectation $K[w] = 3$. Note from the key that the high values of $K[w]$ occur low in the boundary layer.

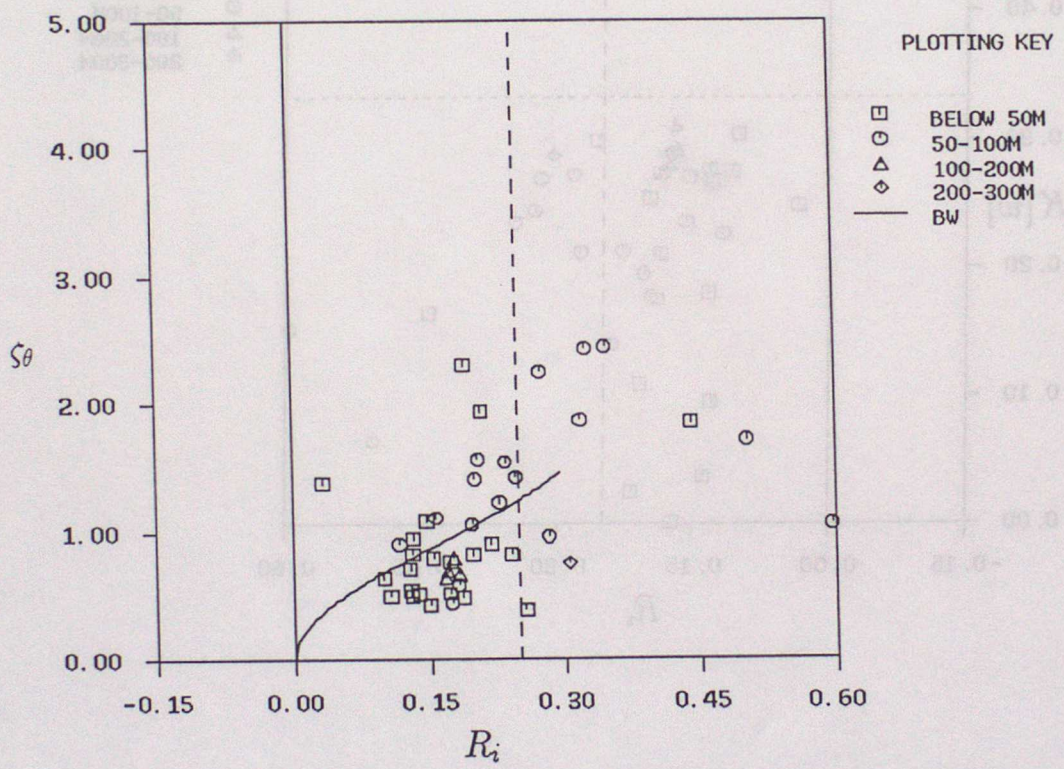

Figure 10a: Non-dimensionalized temperature fluctuation ζ_θ (see text) vs. R_i. Brost-Wyngaard (BW) curve shown for comparison. All plots in Fig. 10 exclude the first run from each day (which is generally transitional) as well as one point from 110393 which showed evidence for contamination of temperature variance. This was in additional to standard quality-control as in 8a.

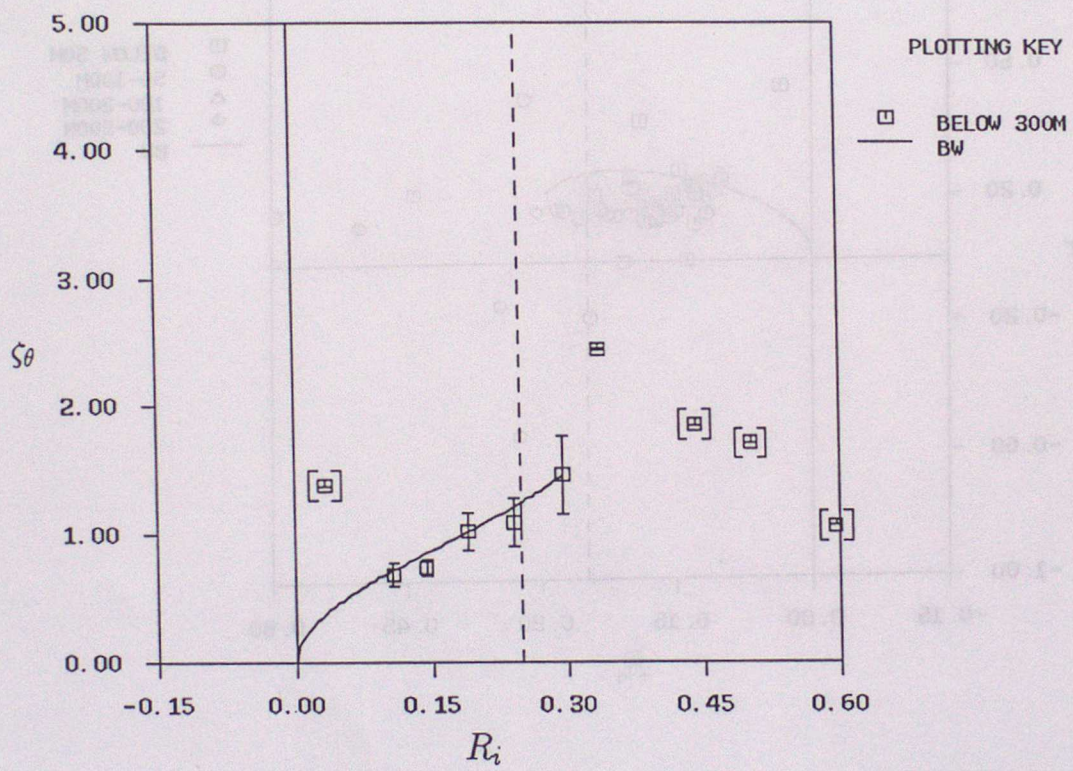

Figure 10b: As 10a, but points below 300m 'binned' by R_i, with standard errors of the bin mean indicated by bars and isolated points bracketed.

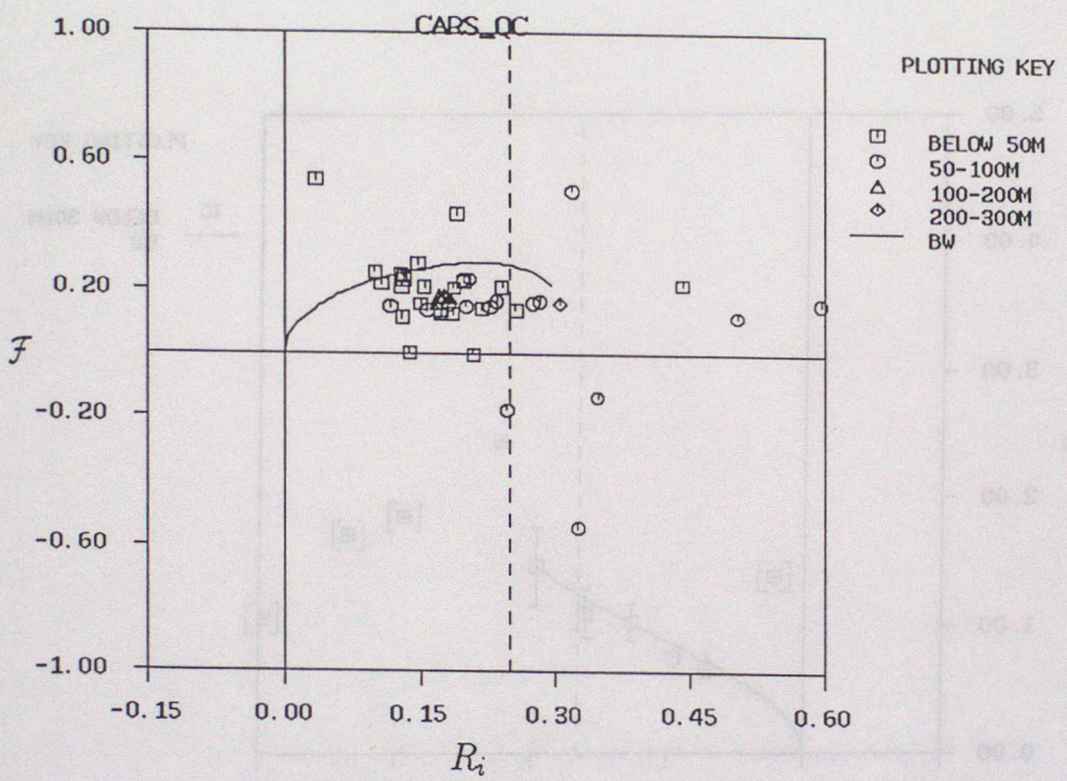

Figure 10c: As 10a, but for nondimensional heat-flux $\mathcal{F}$ (see text).

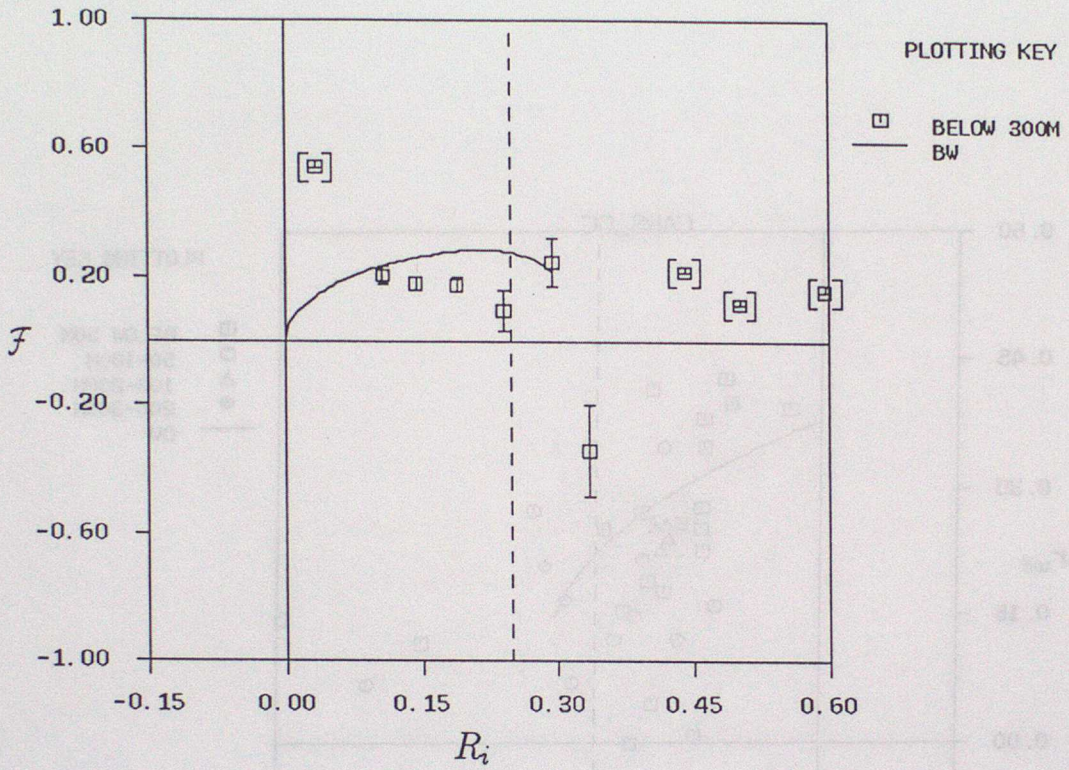

Figure 10d: As 10b, but for nondimensional heat-flux $\mathcal{F}$ (see text).

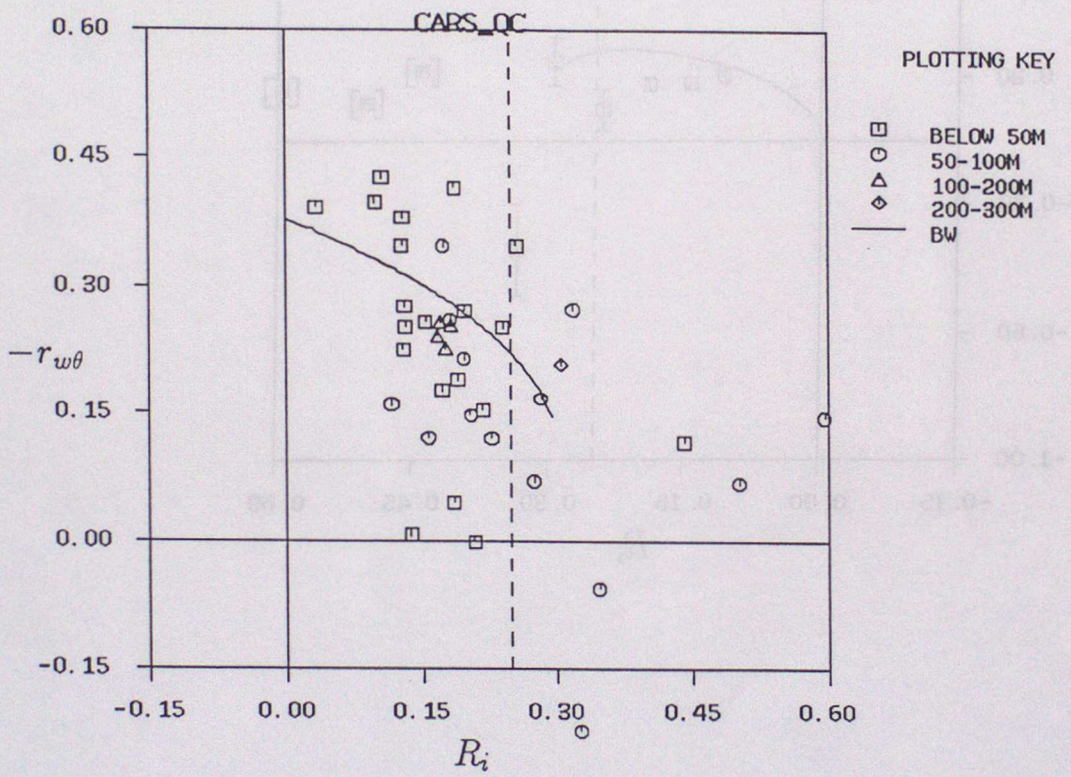

Figure 10e: As 10a, but for the heat-flux correlation coefficient $-r_{w\theta}$.

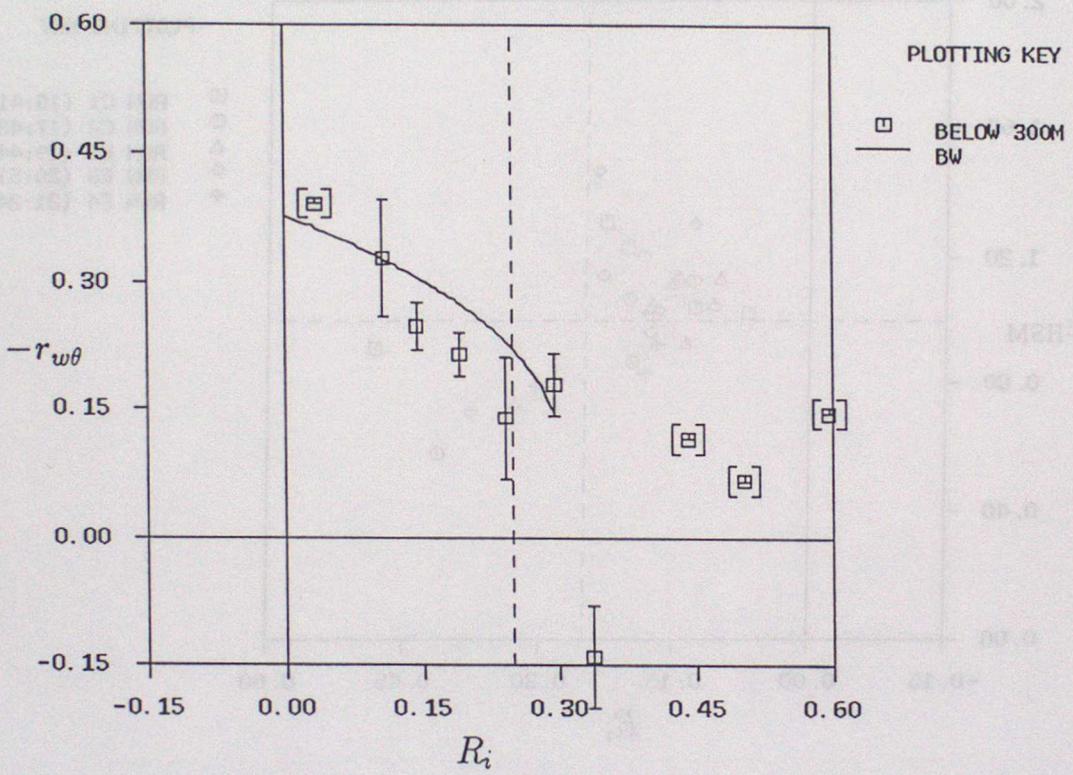

Figure 10f: As 10b, but for the heat-flux correlation coefficient $-r_{w\theta}$.

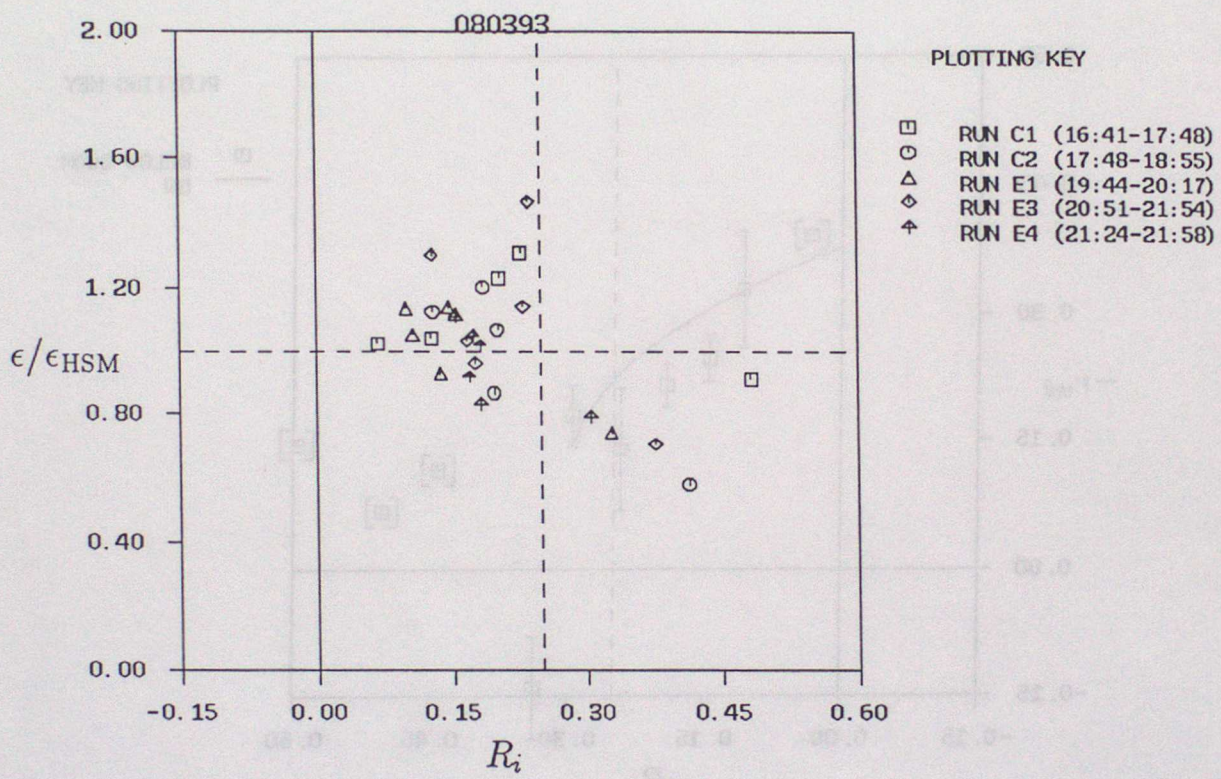

Figure 11: turbulence kinetic energy dissipation ϵ normalized by the HSM prediction (see text), for the 'best' day 080393.

Figure A.1: mixing-length l_m and WTHT/WT, the ratio of slow to fast heat-flux measurements. The curve shows for comparison the hypothesis that WTHT/WT=l_m/(5m+l_m), corresponding roughly to a response length 5m.

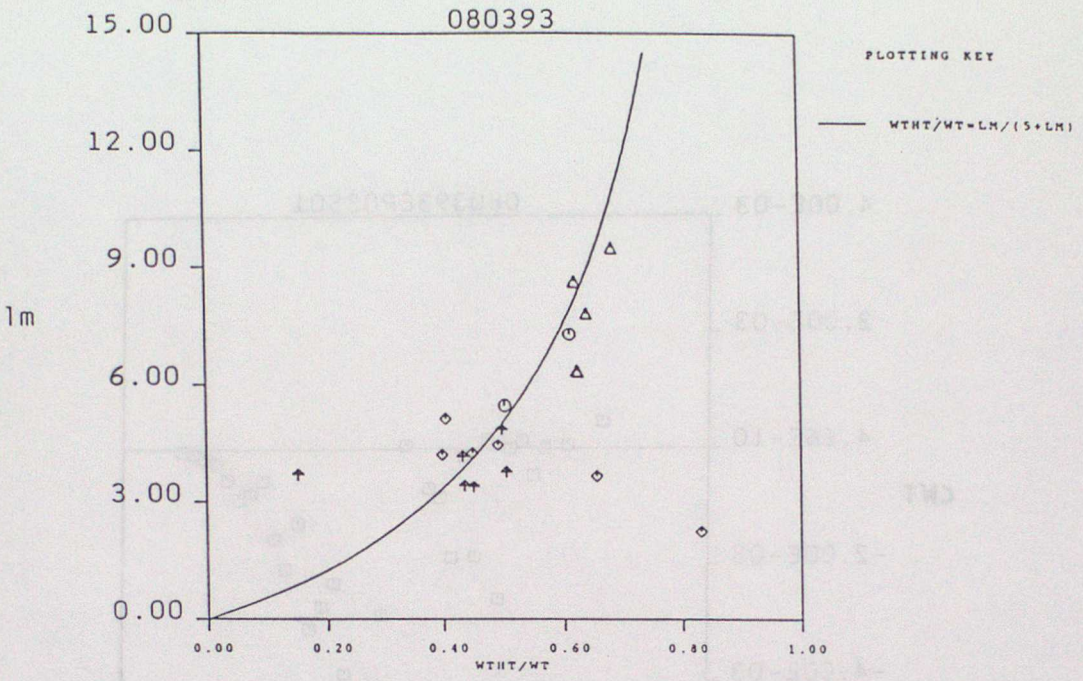

Figure A.2: A 'good' PRT temperature spectrum consistent with inertial subrange $k^{-2/3}$-scaling (guideline shows expected slope) from a probe at 65m.

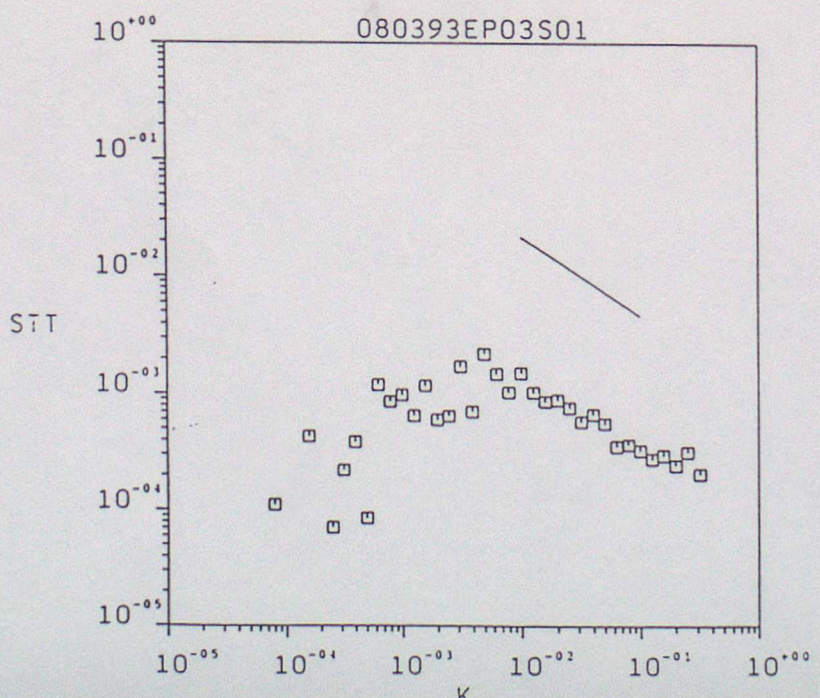

Figure A.3: Heat-flux cospectrum for the same case as A.2.